AD-A041 561 ARMY ELECTRONICS COMMAND FORT MONMOUTH N J F/G 17/7
AN APPROACH GUIDANCE SYSTEM FOR REMOTELY-PILOTED VEHICLES.(U)
JUL 77 N K SHUPE
UNCLASSIFIED ECOM-4503 NL

1 OF 1
AD A041 561

END

DATE FILMED
8-77

2(12)

Research and Development Technical Report

ECOM-4503

AN APPROACH GUIDANCE SYSTEM FOR REMOTELY-PILOTED VEHICLES

Norman K. Shupe

Avionics Laboratory

July 1977

ECOM

US ARMY ELECTRONICS COMMAND FORT MONMOUTH, NEW JERSEY 07703

NOTICES

Disclaimers

The findings in this report are not to be construed as an official Department of the Army position, unless so designated by other authorized documents.

The citation of trade names and names of manufacturers in this report is not to be construed as official Government indorsement or approval of commercial products or services referenced herein.

Disposition

Destroy this report when it is no longer needed. Do not return it to the originator.

UNCLASSIFIED

SECURITY CLASSIFICATION OF THIS PAGE *(When Data Entered)*

REPORT DOCUMENTATION PAGE

READ INSTRUCTIONS BEFORE COMPLETING FORM

1. REPORT NUMBER: ECOM-4503	2. GOVT ACCESSION NO.
3. RECIPIENT'S CATALOG NUMBER	
4. TITLE *(and Subtitle)*: An Approach Guidance System for Remotely-Piloted Vehicles,	5. TYPE OF REPORT & PERIOD COVERED
	6. PERFORMING ORG. REPORT NUMBER
7. AUTHOR(s): Norman K. Shupe	8. CONTRACT OR GRANT NUMBER(s): Technical rept.
9. PERFORMING ORGANIZATION NAME AND ADDRESS: Control Theory Team, Advanced Avionic Systems Tech Area, Avionics Laboratory, Fort Monmouth, NJ	10. PROGRAM ELEMENT, PROJECT, TASK AREA & WORK UNIT NUMBERS: 622202.11.H85.13.00
11. CONTROLLING OFFICE NAME AND ADDRESS: CDR, ECOM, ATTN: DRSEL-VL-F, Fort Monmouth, NJ	12. REPORT DATE: July 1977
	13. NUMBER OF PAGES: 68
14. MONITORING AGENCY NAME & ADDRESS *(if different from Controlling Office)*	15. SECURITY CLASS. *(of this report)*: UNCLASSIFIED
	15a. DECLASSIFICATION/DOWNGRADING SCHEDULE

16. DISTRIBUTION STATEMENT *(of this Report)*

Approved for public release; distribution unlimited

17. DISTRIBUTION STATEMENT *(of the abstract entered in Block 20, if different from Report)*

18. SUPPLEMENTARY NOTES

19. KEY WORDS *(Continue on reverse side if necessary and identify by block number)*

Guidance
Flight Control
Remotely-Piloted Vehicles
Simulation

20. ABSTRACT *(Continue on reverse side if necessary and identify by block number)*

This report develops a guidance formulation with general applicability to the problem of the IFR landing of aircraft of any type; however, the formulation is specialized in this document to the case of a non-decelerating approach to the landing point. The control problem considered is the computer simulation of the automatic landing of a mini-RPV of the delta wing variety.

DD FORM 1 JAN 73 1473 EDITION OF 1 NOV 65 IS OBSOLETE

UNCLASSIFIED

SECURITY CLASSIFICATION OF THIS PAGE *(When Data Entered)*

037 620

TABLE OF CONTENTS

FIGURES

1. INTRODUCTION

As indicated by the title, this report is specifically concerned with the longitudinal approach dynamics of remotely-piloted vehicles. Certain portions of this effort, however, are felt to be applicable to the more general problem of the IFR landing of aircraft of any type. In this report, the "guidance" function specifically refers to the process of defining the longitudinal trajectory of the aircraft through space and time from the point of acquisition to touchdown. If one denotes λ to be the angular error of the aircraft relative to the desired approach path and R the horizontal range to the landing point, then the desired spatial flight path may be described by $\lambda = f(R)$. If $\dot{R}$ denotes the time variation of the horizontal range, the trajectory specification in space and time is completed by $\dot{R} = g(R)$. From the two functional relationships $\lambda = f(R)$ and $\dot{R} = g(R)$, one may uniquely compute the force vector required to fly the trajectory through space and time. If one views the guidance function as specification of the force vector, then the "control" function is quite clearly the process of developing and controlling the aerodynamic, gravitational, and inertial forces acting on the airframe to equal the force vector specified by the guidance function. It is the opinion of the author that the guidance formulation contained in this document has complete application to the general problem of the IFR landing of aircraft of any type; however, the formulation has been specialized in this document to the case of a non-decelerating ($\dot{R}$ = constant) approach to the landing point.

The "control" function is strongly influenced by the nature of the application. For the landing of a piloted-aircraft, the control function emphasis will invariably center upon the landing display, pilot workload, airframe handling qualities and other so-called human factors. For the landing of a remotely-piloted-vehicle, design emphasis will tend toward the auto-pilot as it is the sole means for controlling the forces on the airframe in the prescribed manner. Of paramount importance to these two superficially different control problems is the specific character of the airframe (e.g., helicopter, fixed wing, aspect ratio, drag brakes, wing loading, control power, density altitude, etc.) as well as the nature of the on-board sensors (e.g., rate gyros, accelerometers, vertical gyros, etc.) which are available to modify the specific character of the airframe. The control problem considered within this document is the automatic landing of a mini-RPV of the delta wing variety.

The guidance and control of the lateral/directional motions of the RPV are not considered here. The general approach, particularly in the guidance formulation area, would be very similar to that used for control of the longitudinal motions of the aircraft.

2. GUIDANCE FORMULATION

The genesis of any guidance concept is the calculation of the resultant forces which must act on a vehicle to cause it to move along some desired flight path at some speed of flight. The force of interest here is the one which must act normal to the aircraft spatial velocity to produce the desired flight path curvature. Referring to Figure 1, the path curvature is related to the required incremental acceleration by

$$a = v\dot{\gamma} = v \frac{d\gamma}{dR} \frac{dR}{dt} \tag{2.1}$$

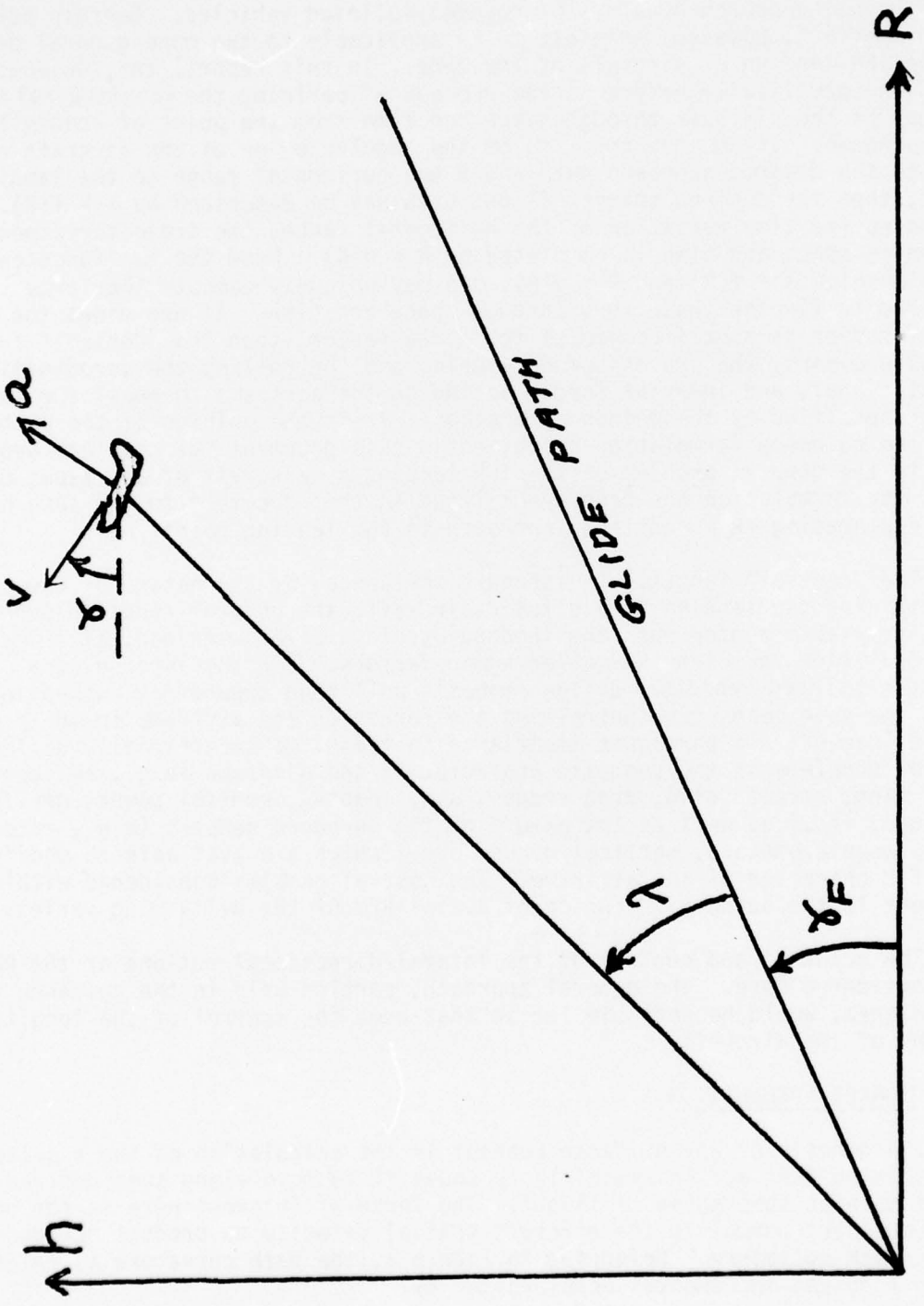

Figure 1. Approach coordinates

The time rate of change of ground range is,

$$\frac{dR}{dt} = \dot{R} = -V \cos \gamma \tag{2.2}$$

Note that $\dot{R}$ is normally a negative number. The inclination of the flight path relative to the horizontal is defined by,

$$\tan \gamma = -\frac{dh}{dR} \tag{2.3}$$

By differentiating (2.3) with respect to the ground range variable (R), one finds;

$$\frac{d\gamma}{dR} = -\cos^2(\gamma) \frac{d^2h}{dR^2} \tag{2.4}$$

Substitution of (2.2) and (2.4) into (2.1) yields,

$$a = v^2 \cos^3 \gamma \frac{d^2h}{dR^2} \tag{2.5}$$

In a typical approach maneuver the flight path angle (γ), the desired flight path angle (γ_F), and the angular error (λ) are small enough to assume SIN( ) = TAN ( ) = ( ) and COS ( ) = 1.

$$a \simeq \dot{R}^2 \frac{d^2h}{dR^2} \tag{2.6}$$

The approach guidance problem is generally more suited to an angular equation formulation rather than a linear displacement formulation. The conversion may be easily accomplished by use of the definition of the angular error (λ),

$$\lambda = \frac{h}{R} - \gamma_F \tag{2.7}$$

Differentiating (2.7) with respect to the range variable (R),

$$\frac{d\lambda}{dR} = \frac{1}{R} \frac{dh}{dR} - \frac{1}{R} \left(\frac{h}{R}\right) \tag{2.8}$$

and then once again,

$$\frac{d^2\lambda}{dR^2} = \frac{1}{R} \frac{d^2h}{dR^2} - \frac{2}{R^2} \frac{dh}{dR} + \frac{2}{R} 2\left(\frac{h}{R}\right) \tag{2.9}$$

Using (2.3) and (2.7), equations (2.8) and (2.9) become,

$$\frac{d}{dR} = -\frac{1}{R} (\gamma + \gamma_F + \lambda) \tag{2.10}$$

And,

$$\frac{d^2\lambda}{dR^2} = \frac{1}{R}\frac{d^2h}{dR^2} - \frac{2}{R}\frac{d\lambda}{dR} \tag{2.11}$$

Rearranging (2.11),

$$\frac{d^2h}{dR^2} = R\frac{d^2\lambda}{dR^2} + 2\frac{d\lambda}{dR} \tag{2.12}$$

and substitution of (2.12) into (2.6) yields,

$$a = \dot{R}^2\left[R\frac{d^2\lambda}{dR^2} + 2\frac{d\lambda}{dR}\right] \tag{2.13}$$

Expression (2.13) relates the acceleration experienced at any range R by a body traveling along a shallow flight path $\lambda = \lambda(R)$, to its ground speed (R) and to the specific nature of the flight path ($d^2\lambda/dR^2$, $d\lambda/dR$) at that range (R).

Quite often one encounters a situation where a basically responsive vehicle must first be controlled, and then guided with precision along some predetermined flight path. The "control" of the vehicle is conventionally associated with its short term behavior while the concept of "guidance" relates to its more long-term behavior. Quite often the dynamics of the control of the vehicle are substantially faster than the guidance dynamics; so much so, that the first-ordered analysis of the two functions may proceed independently. The landing approach of an RPV is of this class of problem. One may take advantage of this fact by assuming a desirable flight path, computing the guidance command required to follow the desirable flight path, and later concern oneself with the details of the autopilot required to follow the guidance command (i.e., the control function).

A stable flight path $\lambda = \lambda(R)$ from the current state of the aircraft ($\lambda = \lambda_1$, $R = R_1$) to the desired landing point ($\lambda = 0$, $R = 0$) should satisfy the following constraints:

1. When $R = 0$, $\lambda = 0$, and $d\lambda/dR = 0$
2. When $R = R_1$, $\lambda = \lambda$, and $\frac{d\lambda}{dR} = -\frac{1}{R_1}(\gamma_1 + \lambda_1 + \gamma_F)$

(2.14)

Note that the current state of the aircraft is designated by the subscript "1." As four arbitrary coefficients are required to satisfy the four endpoint constraints, assume the flight path to be of the well-behaved form,

$$\lambda = C_0 + C_1, R + C_2R^{n+1} + C_3 R^{n+2} \tag{2.15}$$

The quantity n is a constant parameter which will be used for adjusting system gain at acquisition. The constraints at $R = 0$ immediately require $C_0 = C_1 = 0$. The remaining expressions for C_2 and C_3 follow from,

$$\lambda_1 = C_2 R_1^{n+1} + C_3 R_1^{n+2} \tag{2.16}$$

$$-\frac{1}{R_1}(\gamma_1 + \lambda_1 + \gamma_F) = (n+1)\,C_2\,R_1^{\,n} + (n+2)\,C_3\,R_1^{\,n+1} \tag{2.17}$$

Simultaneous solution of the algebraic equations (2.16) and (2.17) yields,

$$C_2 = \frac{1}{R_1^{\,n+1}}\left[(n+3)\,\lambda_1 + \gamma_1 + \gamma_F\right] \tag{2.18}$$

$$C_3 = \frac{1}{R_1^{\,n+2}}\left[-(n+2)\cdot\lambda_1 - \gamma_1 - \gamma_F\right] \tag{2.19}$$

The nominal flight path from the current state of the aircraft ($R = R_1$, $\lambda = \lambda_1$, $\gamma = \gamma_1$) to the landing state of the aircraft ($R = o$, $\lambda = o$, $\gamma = \gamma_F$) is,

$$\lambda = \left(\frac{R}{R_1}\right)^{n+1}\left[(n+3)\,\lambda_1 + \gamma_1 + \gamma_F\right] + \left(\frac{R}{R_1}\right)^{n+2}\left[-(n+2)\,\lambda_1 - \gamma_1 - \gamma_F\right] \tag{2.20}$$

Also,

$$\frac{d\lambda}{dR} = (n+1)\left(\frac{R}{R_1}\right)^{n}\left(\frac{1}{R_1}\right)\left[(n+3)\,\lambda_1 + \gamma_1 + \gamma_F\right] + (n+2)\left(\frac{R}{R_1}\right)^{n+1}\left(\frac{1}{R_1}\right)\left[-(n+2)\,\lambda_1 - \gamma_1 - \gamma_F\right] \tag{2.21}$$

and,

$$\frac{d^2\lambda}{dR^2} = (n)(n+1)\left(\frac{R}{R_1}\right)^{n-1}\left(\frac{1}{R_1}\right)^2\left[(n+3)\,\lambda_1 + \gamma_1 + \gamma_F\right] + (n+1)(n+2)\left(\frac{R}{R_1}\right)^{n}\left(\frac{1}{R_1}\right)^2 = \left[-(n+2)\,\lambda_1 - \gamma_1 - \gamma_F\right] \tag{2.22}$$

Substituting (2.21) and (2.22) into (2.13) yields,

$$a = \dot{R}^2\left\{(n+1)(n+2)\left(\frac{R}{R_1}\right)^{n}\left(\frac{1}{R_1}\right)\left[(n+3)\,\lambda_1 + \gamma_1 + \gamma_F\right] + (n+2)(n+3)\left(\frac{R}{R_1}\right)^{n+1}\frac{1}{R_1}\left[-(n+2)\,\lambda_1 - \gamma_1 - \gamma_F\right]\right\} \tag{2.23}$$

Again, (2.23) describes the acceleration profile required to fly the nominal flight path from the current state ($R = R_1$, $\gamma = \gamma_1$, $\lambda = \lambda_1$) to the landing state. The current command (a_C) results from using $R = R_1$, in (2.23). For current guidance command generation purposes, the subscripts "1" are dropped as all variables are current. The resultant guidance command is,

$$a_C = \frac{\dot{R}^2}{R} (n + 2) \left[-(n + 3) \lambda - 2\gamma - 2\gamma_F\right] \tag{2.24}$$

In effect, the aircraft never attempts to return to any previous nominal flight path, but instead, continually recomputes a new nominal path from the current state. As the measurable quantities are λ and $\dot{\lambda}$, use of (2.10) and $\dot{\lambda} = \dot{R}\, d\lambda/dR$ yields,

$$\dot{\lambda} = \frac{-\dot{R}}{R} (\lambda + \gamma + \gamma_F) \tag{2.25}$$

Use of (2.25) in (2.24) yields,

$$a_C = (-2\dot{R}) (n + 2) (\dot{\lambda}_C - \dot{\lambda}) \tag{2.26}$$

where

$$\dot{\lambda}_C = \frac{R (n + 1)}{2} \left(\frac{\lambda}{R}\right) \tag{2.27}$$

Expression 2.27 will be used in a later section to command limit $\dot{\lambda}$ and hence the maximum descent angle (γ). The acceleration command of (2.26) can be manipulated into a second-ordered, linear differential equation by use of (2.13).

$$\dot{R}^2 \left(R \frac{d^2\lambda}{dR^2} + 2 \frac{d\lambda}{dR}\right) = -2\dot{R} (n + 2) \left[\frac{\dot{R}(n + 1)}{2} \frac{\lambda}{R} - \dot{R} \frac{d\lambda}{dR}\right] \tag{2.28}$$

Rearrangement of (2.28) yields,

$$R^2 \frac{d^2\lambda}{dR^2} - 2 (n + 1) R \frac{d\lambda}{dR} + (n + 1) (n + 2) \lambda = 0 \tag{2.29}$$

The particular solution to 2.29 which satisfies the desired boundary conditions is obviously equation 2.20. (If this is not obvious, the reader should recall that the solution 2.20 was the assumed starting point.) Equation 2.29 will be used in the next section on limiting system gain.

Figure 2 depicts the response of 2.26 for acquisition of the glide slope ($\gamma_F = 4^o$) at R = 3,000 feet, with an initial altitude error of 100 feet (λ = 1/30 radian). The range and altitude error channels are dynamically rescaled at R = 300 feet for accuracy. The inherent stability of 2.26 for small values of R is quite clear.

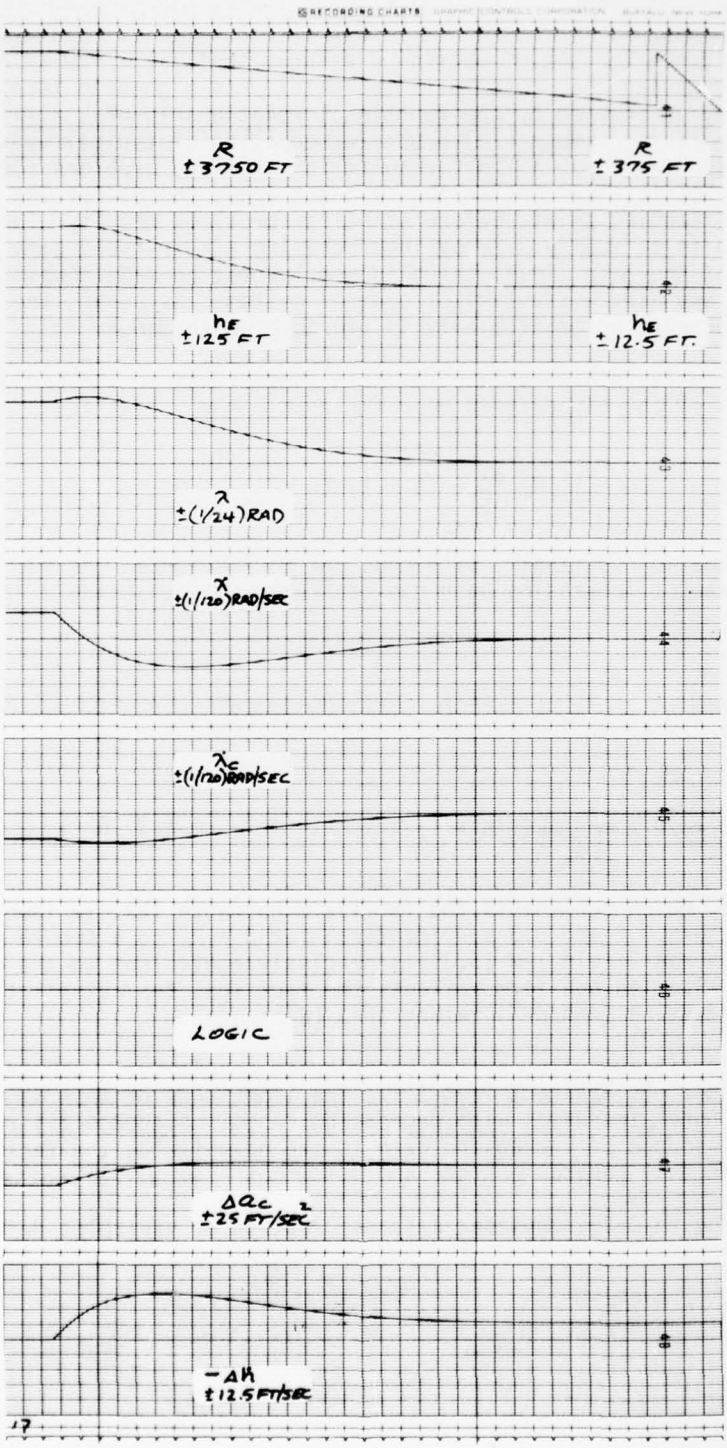

Figure 2. Ideal system response (n = 5, γ_F = 4°, $\dot{R}$ = -85 ft/sec)

3. SYSTEM GAIN CONTROL

The guidance concept of section 2 assures that $\lambda = \dot{\lambda} = 0$ as R goes to zero, by increasing the system gain to infinity as R goes to zero. Ideal system stability is insured by the functional relationship of $\lambda = [\lambda(R)]$ to R as R goes to zero (i.e., $LIM_{R\to 0}(\lambda/R) = 0$. Introduction of typical dynamic lags in aircraft response (i.e., $a \neq a_c$) results in stability problems somewhere near the landing point. The smaller the response lags, the nearer the aircraft can approach the landing point, before stability problems result. The intent of this section is to modify 2.26 by incorporating a near-field gain control. By adjustment of the gain limit, the guidance law may be made compatible with the dynamics of any aircraft/autopilot control system. As usual, the price one pays for adequate system stability is degraded performance.

The author's initial attempt at gain control was to use an altered form of 2.29 to control the aircraft in near field ($R \leq R_m$). That is,

$$R_m^2 \frac{d^2\lambda}{dR^2} - 2(n+1) R_m \frac{d\lambda}{dR} + (n+1)(n+2)\lambda = 0 \qquad (3.1)$$

The above equation is linear, with constant coefficients. As such, the most obvious source of increasing gain has been eliminated. Using 2.13 in 3.1 one finds;

$R \geq R_m$

$$a_c = 2(n+2)\dot{R}\dot{\lambda} - (n+1)(n+2)\dot{R}^2(\lambda/R) \qquad (3.2)$$

$R \leq R_m$

$$a_c = 2\dot{R}\dot{\lambda} + \left(\frac{R}{R_m}\right)\left[2(n+1)\dot{R}\dot{\lambda} - \frac{(n+1)(n+2)R^2\lambda}{R_m}\right] \qquad (3.3)$$

Equation 3.2, which represents the far-field guidance law, is identical to 2.26. Equations 3.2 and 3.3 are identical for $R = R_m$ so a smooth transition is assured. The near-field law (3.3) is precisely equivalent to the differential equation (3.1). Its odd form reflects the fact that the autopilot will control normal acceleration (d^2h/dR^2) rather than ($d^2\lambda/dR^2$).

The aircraft/autopilot system contributes a relatively constant dynamic lag in d^2h/dR^2. As apparent from 2.11, the importance of this lag to the vehavior of $d^2\lambda/dR^2$, increases with decreasing range. Although 3.1 removes the most obvious source of increasing gain in the near field, the fact that the autopilot can only control d^2h/dR^2 and not $d^2\lambda/dR^2$, required another approach.

Returning to 2.29, consider a transformation of variables defined by

$$\lambda = \frac{h}{R} - \gamma_F = \frac{h\varepsilon}{R} \qquad (3.4)$$

Differentiation with respect to the ground range (R) yields,

$$\frac{d\lambda}{dR} = \frac{1}{R}\left[\frac{dh_\varepsilon}{dR} - \frac{h_\varepsilon}{R}\right] \tag{3.5}$$

and once again

$$\frac{d^2\lambda}{dR^2} = \frac{1}{R}\left[\frac{d^2h_\varepsilon}{dR^2} - \frac{2}{R}\frac{dh_\varepsilon}{dR} + \frac{2h_\varepsilon}{R}\right] \tag{3.6}$$

Substitution of 3.5 and 3.6 into 2.29 results in,

$$R^2\frac{d^2h_\varepsilon}{dR^2} - 2(n+2)R\frac{dh_\varepsilon}{dR} + (n+2)(n+3)h_\varepsilon = 0 \tag{3.7}$$

The above equation describes the ideal response of the guidance law in terms of altitude error relative to the desired straight line approach path of inclination γ_F. It is completely equivalent to 2.29 which relates system response in terms of the angular error (λ) rather than the altitude error (h_ε).

Near field guidance will be based upon the following linear differential equation with <u>constant</u> coefficients obtained from 3.7,

$$R_m^2\frac{d^2h_\varepsilon}{dR^2} - 2(n+2)R_m\frac{dh_\varepsilon}{dR} + (n+2)(n+3)h_\varepsilon = 0 \tag{3.8}$$

Since d^2h/dR^2 is equal to d^2h_ε/dR^2, the first term is measurable and, in fact, under control of the autopilot. The near-field guidance law formulation will be completed by elimination of dh_ε/dR and h_ε in favor of the measurable quantities $\dot{\lambda}$ and λ.

Using 3.4 and 3.5 in 3.8, one finds,

$$\frac{d^2h_\varepsilon}{dR^2} = 2(n+2)\left(\frac{R}{Rm}\right)\left\{\left[1 - \frac{(n+3)}{2}\frac{R}{Rm}\right]\left(\frac{\lambda}{R}\right) + \frac{d\lambda}{dR}\right\} \tag{3.9}$$

or

<u>$R \leq Rm$</u>

$$a_c = -2(n+2)(\dot{R})\left(\frac{R}{Rm}\right)(\dot{\lambda}_c - \dot{\lambda}) \tag{3.10}$$

where,

$$\dot{\lambda}_c = (-\dot{R})\left[1 - \frac{(n+3)}{2}\left(\frac{R}{R_m}\right)\right]\left(\frac{\lambda}{R}\right) \tag{3.11}$$

Expressions 3.10 and 3.11 are equal to the far-field guidance expressions 2.26 and 2.27 when R = Rm insuring a smooth transition. A single guidance expression encompassing both the near-field and far-field laws is,

$$a_c = (-2\dot{R})(n+2)\left(\frac{R}{R'}\right)(\lambda_c - \dot{\lambda}) \tag{3.12}$$

where,

$$\dot{\lambda}_c = (-\dot{R})\left[1 - \left(\frac{n+3}{2}\right)\left(\frac{R}{R'}\right)\right](\lambda/R) \tag{3.13}$$

and,

$$R' = R \qquad \text{if} \qquad R \geq R_m$$

$$R' = R_m \qquad \text{if} \qquad R \leq R_m$$

The guidance law operates in the far-field on the measured angular information with increasing gain as the range decreases. At some range ($R = R_m$) the guidance concept, in effect, converts the measured angular information (λ, $\dot{\lambda}$) to its linear equivalent (h_ε, $\dot{h}_\varepsilon$) and then freezes the system gain at the R_m value. If the system is stable at a range R_m, it will be stable for all $R \leq R_m$. One should realize, however, that the system will respond to a gust input which occurs at <u>any</u> range $R < R_m$ with the same urgency as if it had occurred at $R = R_m$. One's obvious goal then, is to make sure that the system achieves its <u>maximum</u> tolerable gain at $R = R_m$ to minimize the effects of near-field disturbances due to wind gusts and manual tracking errors.

To quantify the near-field gust response of this guidance formulation, consider the response of 3.8 to an aerodynamically-produced disturbance. Later in this document, the effects of the autopilot design upon gust alleviation/amplification will be addressed. There, one will find that the pitch attitude behavior of the stabilized airframe in response to a normal wind gust (ΔW_G) disturbance controls the degree of gust amplification/alleviation (i.e., the resulting $\dot{h}$ or γ response). If the airframe does not pitch, a wind gust of magnitude ΔW_G will soon translate the airframe at that rate (i.e., $\dot{h} = \Delta W_G$). The time lag to achieve this rate is predominately the "short period mode" of the airframe. For the analysis to follow, this time lag is ignored and equation 3.8 is subjected to the following initial conditions when t = 0;

$$h_\varepsilon = 0, \quad \frac{dh_\varepsilon}{dt} = \Delta W_G \tag{3.14}$$

where ΔW_G is positive for an up-gust. The following change of variables is convenient for analytical purposes.

$$R_T = R_D - R \tag{3.15}$$

where R_D is the range from the desired landing point at which the wind gust occurs, and R_T is the transposed range variable. Equation 3.8 becomes,

$$R_m^2 \frac{d^2h_\varepsilon}{dR_T^2} + 2(n+2) R_m \frac{dh_\varepsilon}{dR_T} + (n+2)(n+3) h_\varepsilon = 0 \qquad (3.16)$$

subject to the initial conditions, at $R_T = 0$,

$$h_\varepsilon = 0, \quad \frac{dh_\varepsilon}{dR_T} = \left(\frac{\Delta W_G}{-\dot{R}}\right) = \Delta\alpha_G \qquad (3.17)$$

The variable $\Delta\alpha_G$ is physically the change in airframe angle of attack produced by the wind gust (i.e., $\Delta\gamma(0) = \Delta\alpha_G$ due to $\Delta\theta$ being assumed equal to zero). Since equation 3.6 is linear with constant coefficients, its solution is easily obtained by Laplace transform techniques. Using,

$$\mathcal{L}[f^m(t)] = S^m F(s) - S^{m-1} f(0) - S^{m-2} f'(0)\ldots \qquad (3.18)$$

The Laplace transform of the solution is

$$H_E(S) = \frac{\Delta\alpha_G}{S^2 + \frac{2(n+2)}{R_m} S + \frac{(n+2)(n+3)}{R_m^2}} \qquad (3.19)$$

The nondimensional solution is,

$$\bar{h}_E(\bar{R}_T) = \left(\frac{1}{\sqrt{n+2}}\right) e^{-(n+2)\bar{R}_T} \text{SIN}(\sqrt{n+2}\ \bar{R}_T) \qquad (3.20)$$

where

$$\bar{h}_E(\bar{R}_T) = \frac{h_E(R_T/R_m)}{\Delta\alpha_G R_m} \qquad (3.21)$$

Figure 3 is a plot of (3.20) for a family of values of the parameter (n). This figure indicates that with R_m held constant, increases in the parameter (n) decrease the maximum error amplitude (h_E). The worst case location for the arresting gear ($R = 0$) is where the peak gust response occurs ($\bar{R}_T = \bar{R}_{TMAX}$) for any value of the parameter (n). As indicated previously, the intent is to cause the system gain to be at its maximum tolerable value at $R = R_m$. This in effect specifies a single value for n so that conclusions made concerning variations in n, with R_m held constant, are invalid. A change in n demands a change in R_m to hold the system gain constant. Consider the undamped natural frequency of oscillation (W_H) and damping factor (E_H) of 3.16.

$$W_H = \frac{\sqrt{(n+2)(n+3)}}{R_m} \qquad (3.22)$$

$$E_H = \sqrt{\frac{n+2}{n+3}} \qquad (3.23)$$

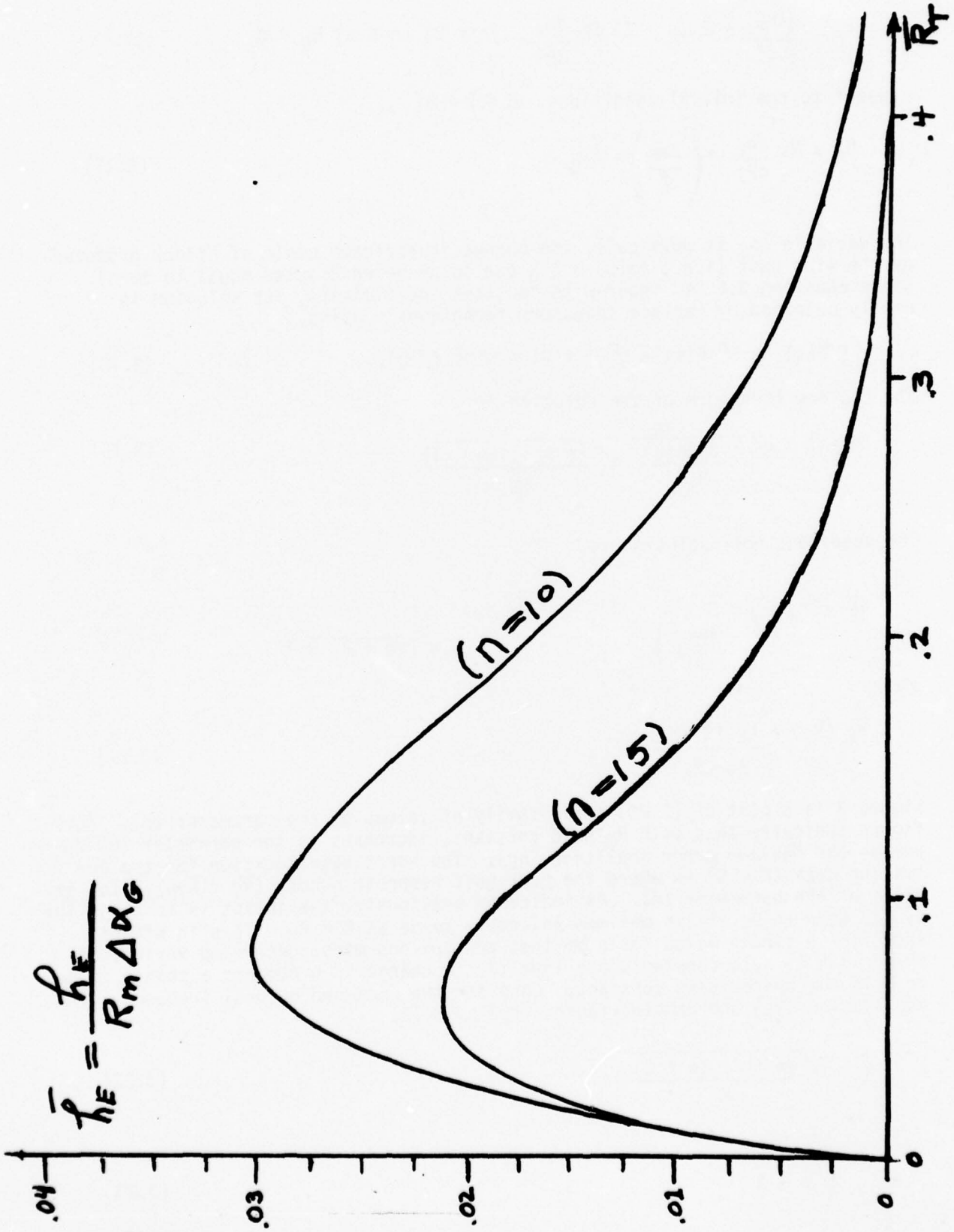

Figure 3. Idealized altitude error response to a vertical gust

If one makes an a'priori assumption that $R_m \sim 1000$ feet and $n \sim 10$ are typical, then one may approximate (3.22) and (3.23) by,

$$W_H \sim \frac{n+2}{R_m} \tag{3.24}$$

$$E_H \sim 1 \tag{3.25}$$

The frequency of oscillation (W_H) best characterizes the concept of system gain and stability so that the desire is to examine the behavior of (3.20) with W_N held constant rather than R_m.

The peak value for $\bar{h}_E$ ($\bar{R}_T$) results from first differentiating (3.20) with respect to $\bar{R}_T$, setting the result equal to zero, and solving the resultant equation for the value of $\bar{R}_T$ at which the peak occurs ($\bar{R}_{TMAX}$)

$$\bar{R}_{TMAX} = \frac{\tan^{-1}(1/\sqrt{n+2})}{\sqrt{n+2}} \tag{3.26}$$

Again assuming $n \sim 10$,

$$\bar{R}_{TMAX} \simeq \frac{1}{n+2} \tag{3.27}$$

or,

$$R_{TMAX} \simeq \frac{R_m}{n+2} \simeq W_H^{-1} \tag{3.28}$$

Substituting (3.27) into (3.20) one finds the peak nondimensional amplitude ($\bar{h}_{EMAX}$)

$$\bar{h}_{EMAX} \simeq \frac{1}{\sqrt{n+2}}\, e^{-1} \,\text{SIN}\,(1/\sqrt{n+2}) \tag{3.29}$$

Again using $n \sim 10$

$$\bar{h}_{EMAX} \simeq \frac{e^{-1}}{n+2}$$

or,

$$\frac{h_{EMAX}}{\Delta\alpha_G} = \frac{P_{me}^{-1}}{n+2} = e^{-1}\, W_H^{-1} \tag{3.30}$$

For the autopilot control system discussed in a later section, stability considerations dictate that the minimum value of W_H^{-1} is on the order of 60 feet. From (3.30), the worst case gust response for the RPV system of this document is approximately 21 feet of error per radian of $\Delta\alpha_G$ or at an approach speed of 85 feet per second, approximately 1/4 foot of error per foot per second of ΔW_G.

As indicated by (3.28) and (3.30), the gust characteristics of the guidance law during the final approach phase ($R \leq R_m$) are only a function of the chosen spatial period (W_H^{-1}) of the system. It is suggested here that the choice of the particular combination of n and R_m to achieve this chosen spatial period ($W_H^{-1} \sim 60$ feet) be influenced by two considerations. These are (1) the amount of time ($- R_m/\dot{R}$) desired for high gain, concentrated tracking in the final approach phase and (2) the system gain at acquisition ($R \sim 3000$ feet). For the present, judgment (Figure 4) was used to select the $R_m = 1000$ feet, n = 15 option for this brief automated simulation test. This allows about 12 seconds for the final approach phase and reduces acquisition system again (feet per second^2 of commanded acceleration per radian of measured angular error λ) by a factor of 3 from its value at initiation of the final approach phase.

Figures 5 through 8 depict the gust response of 3.13 without gain limiting (i.e., $R_m = 0$), when subjected to an upgust ($\Delta W_G = -\dot{R}\Delta\alpha_G = 5$ FPS) at several ranges. The system is initially trimmed on the descent path and is perturbed from this path by the upgust. Since the assumption of $\Delta\theta = 0$ and initially $\Delta\dot{h} = \Delta W_G$ are retained, the associated step change in $\dot{\lambda}$ is clear. Since the system gain is continually increasing, the peak Δh_E decreases for decreasing range. Although Figure 3 is only truly valid for values of R less than R_m, use of $R_m = R_D$ gives a good approximation to the results of Figures 5 through 8 where $R_m = 0$. For example, from Figure 5, the peak altitude error is $\Delta h_E = 4$ feet. From Figure 3 for $R_m = R_D = 3000$ feet, the predicted value is $\Delta h_E = 3.7$ feet ($\Delta h_E = 0.021\ \Delta\alpha_G$ RD). As indicated by the nondimensional results, the peak h_E remains approximately proportional to the range (R_D) at which the excitation occurred (e.g., 4 feet at $R_D = 3000$ feet, 3 feet at $R_D = 2250$ feet, 2 feet at $R_D = 1500$ feet and 1 foot at $R_D = 750$ feet as shown by Figures 5 through 8).

Figures 9 through 12 depict the ideal system gust response with gain limiting. Figures 9 and 10 were computed with $R_m = 3000$ feet and demonstrate the desired invarient Δh_E response for all values of $R \leq Rm$. These two traces should be compared with Figure 5 ($R_m = 0$) where the disturbance was applied at $R_D = 3000$ feet. Figures 11 and 12 were computed with $R_m = 1000$ feet and demonstrate the ideal system response for the suggested n = 14, $R_m = 1000$ foot design configuration. For the gust response of the design configuration for $R > R_m$, one should refer to Figures 5, 6, and 7 as gain limiting is not in effect for $R > R_m$.

Again, it should be emphasized that the preceding results for $\Delta\theta = 0$ represent the worst case as far as gust sensitivity is concerned. When the airframe is free to respond in pitch attitude to a ΔW_G disturbance, the peak Δh_E will decrease.

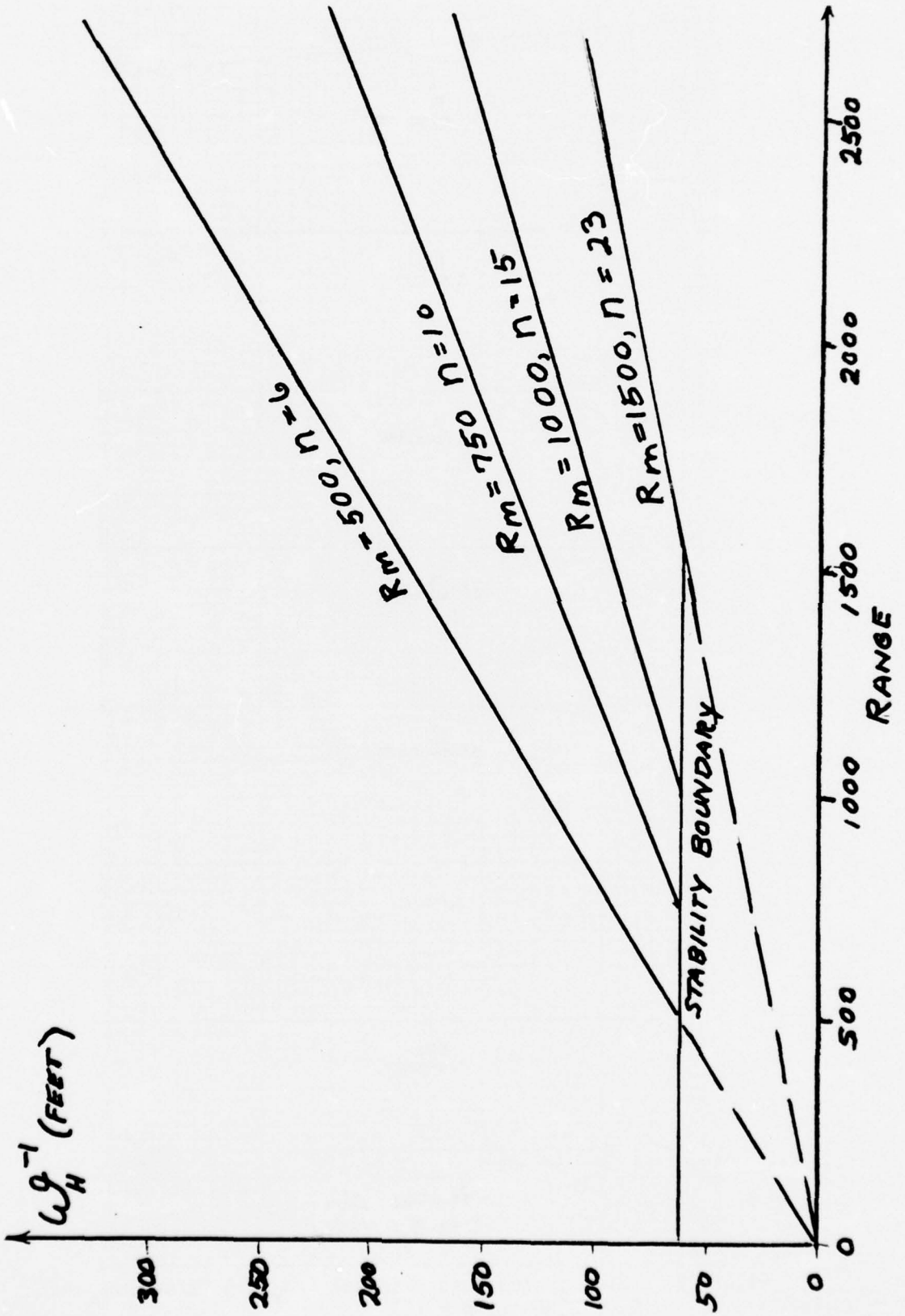

Figure 4. Spatial period of normal acceleration guidance law

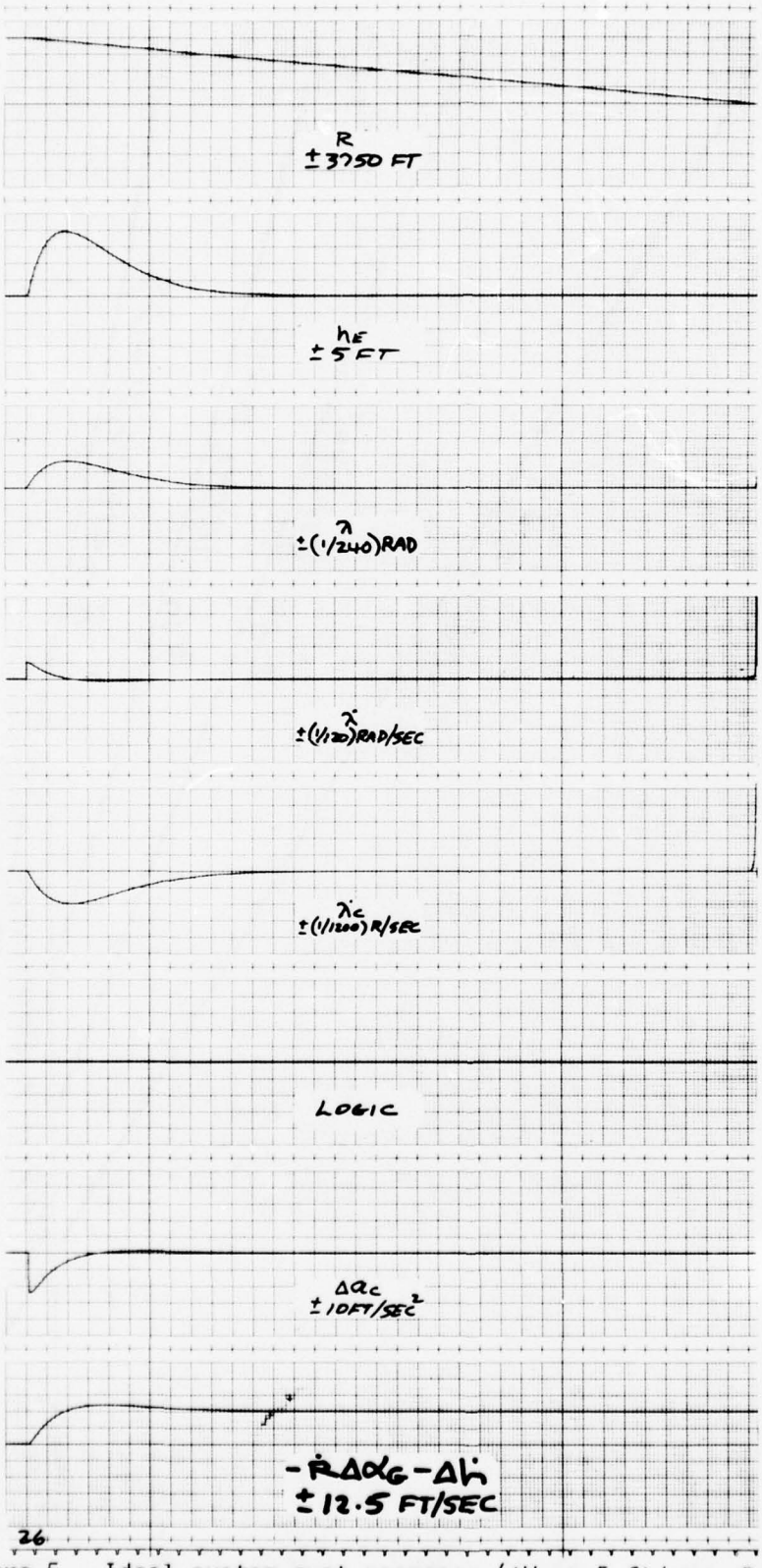

Figure 5. Ideal system gust response (ΔW_G = 5 ft/sec, R_m = 0, R_D = 3000 ft, n = 15)

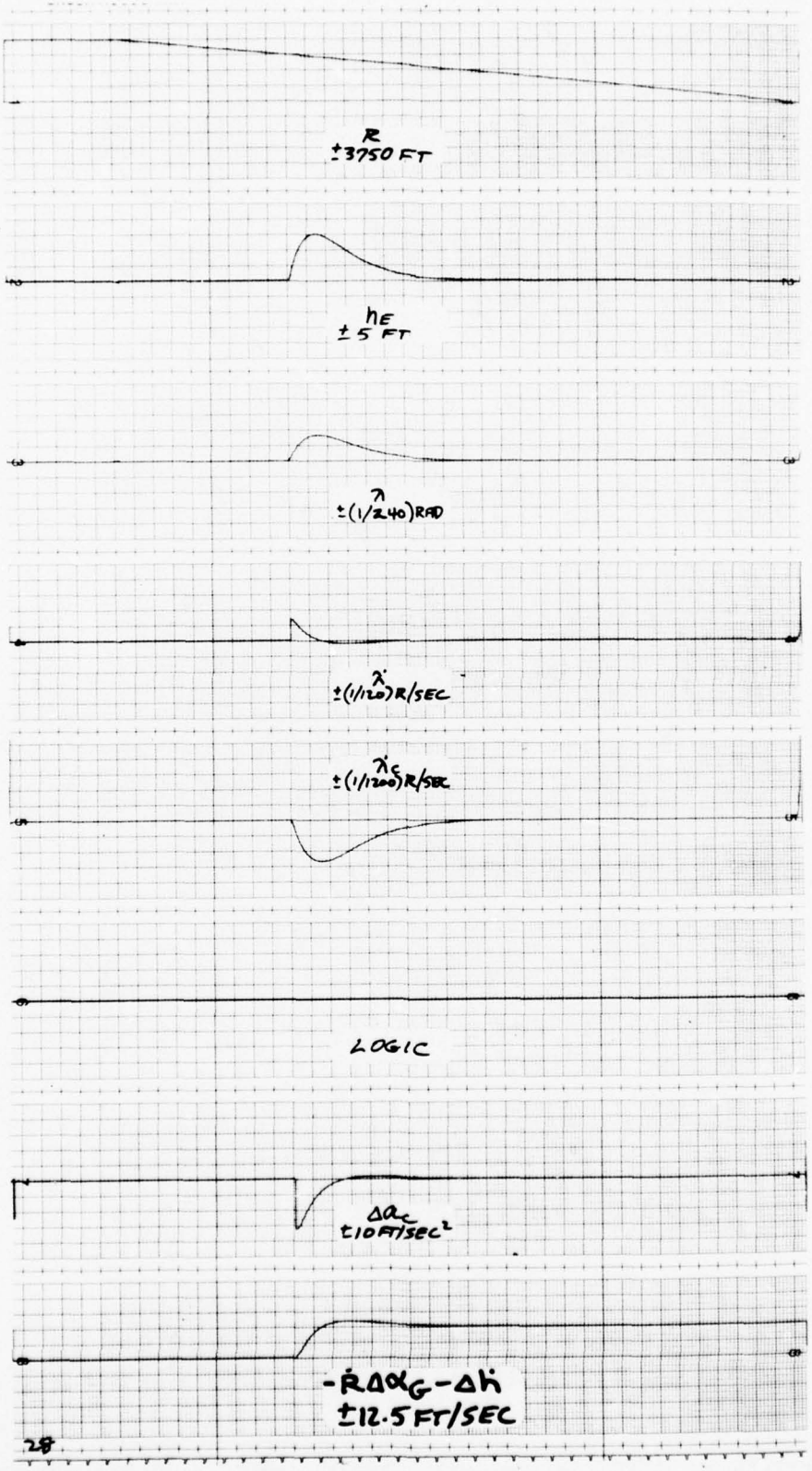

Figure 6. Ideal system gust response (ΔW_G = 5 ft/sec, R_m = 0, R_D = 2250 ft, n = 15)

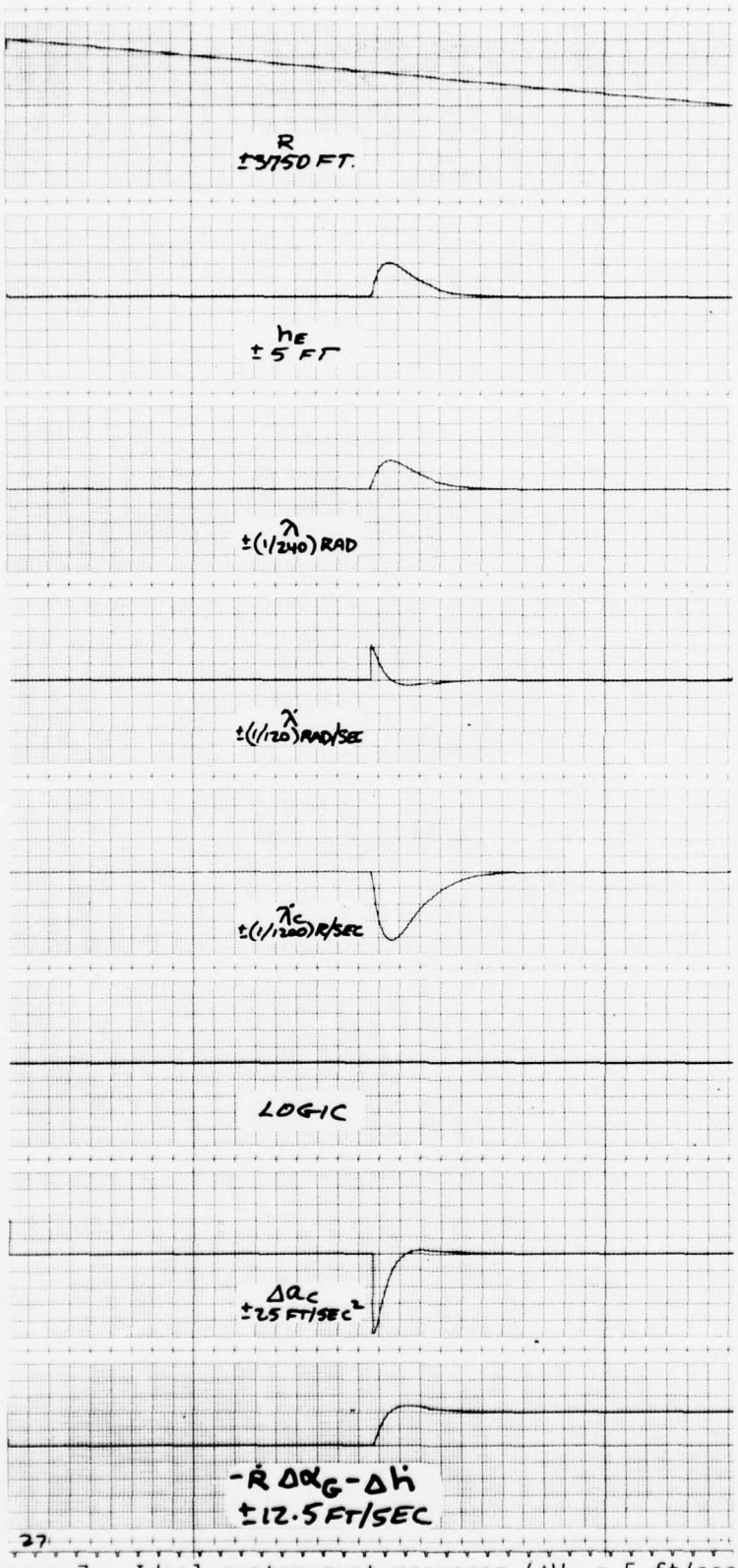

Figure 7. Ideal system gust response (ΔW_G = 5 ft/sec, R_m = 0, R_D = 1500 ft, n = 15)

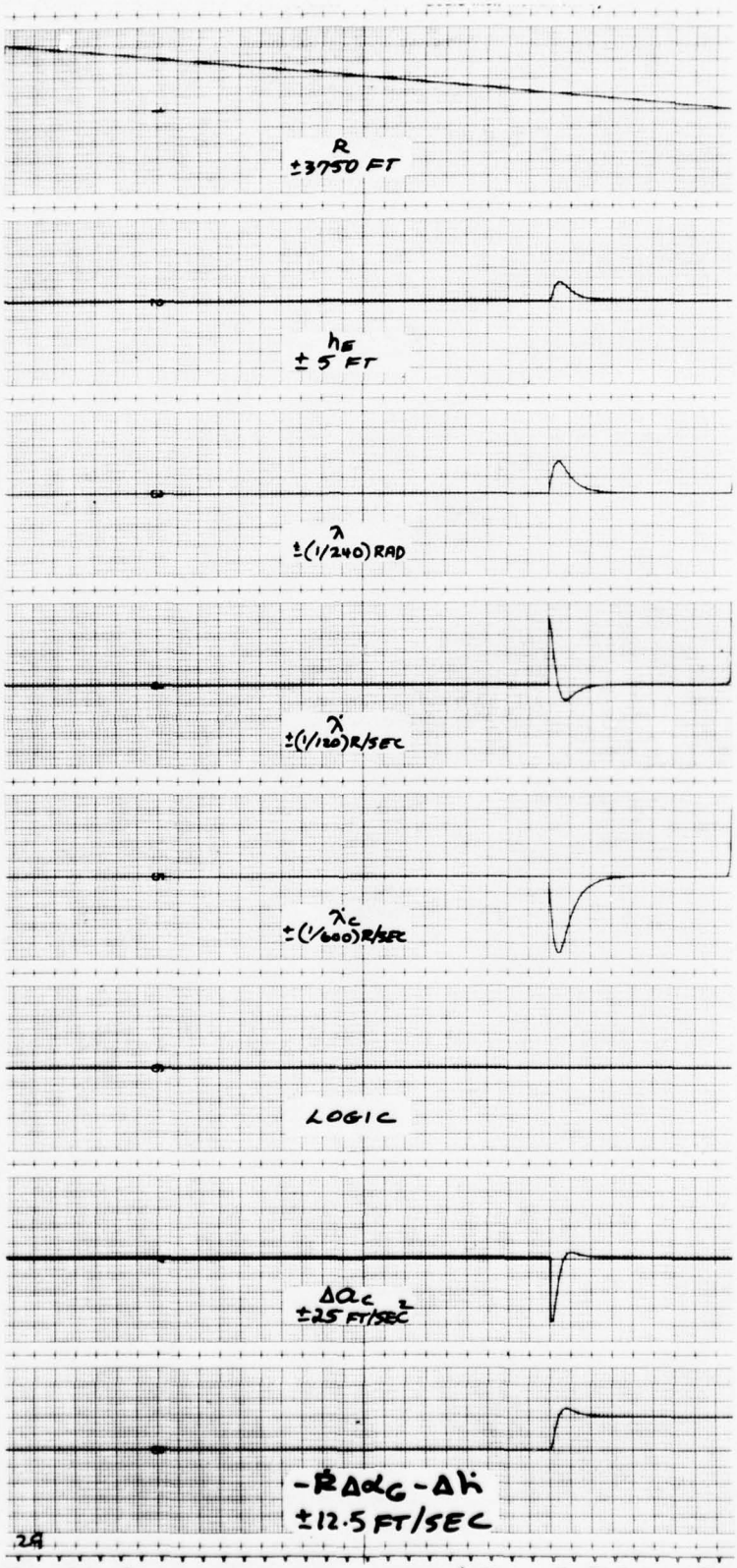

Figure 8. Ideal system gust response (ΔW_G = 5 ft/sec, R_m = 0, R_D = 750 ft, n = 15)

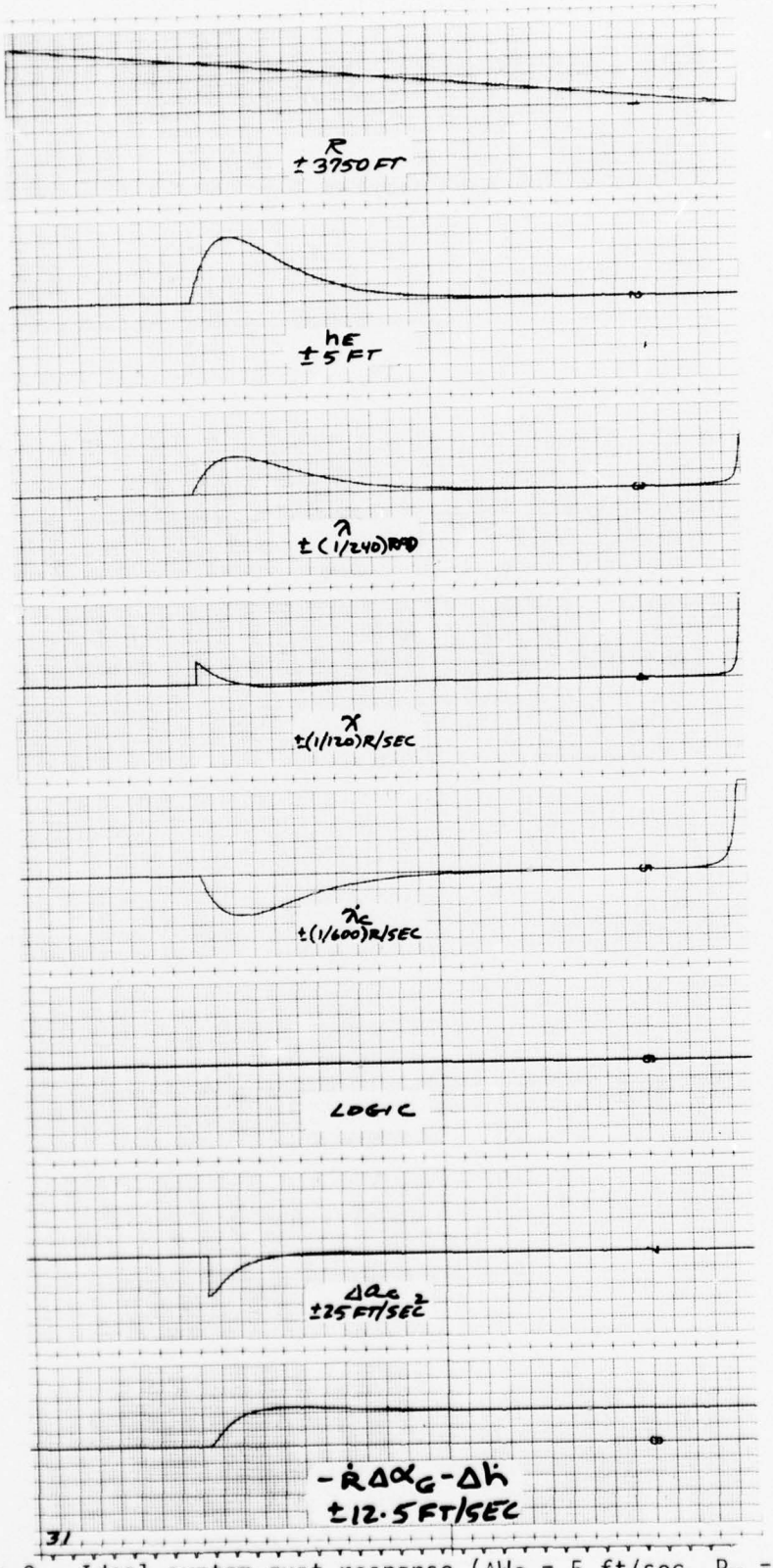

Figure 9. Ideal system gust response (ΔW_G = 5 ft/sec, R_m = 3000 ft, R_D = 2250 ft, n = 15)

Figure 2. Ideal system response (n = 5, $\gamma_F = 4^o$, $\dot{R}$ = -85 ft/sec)

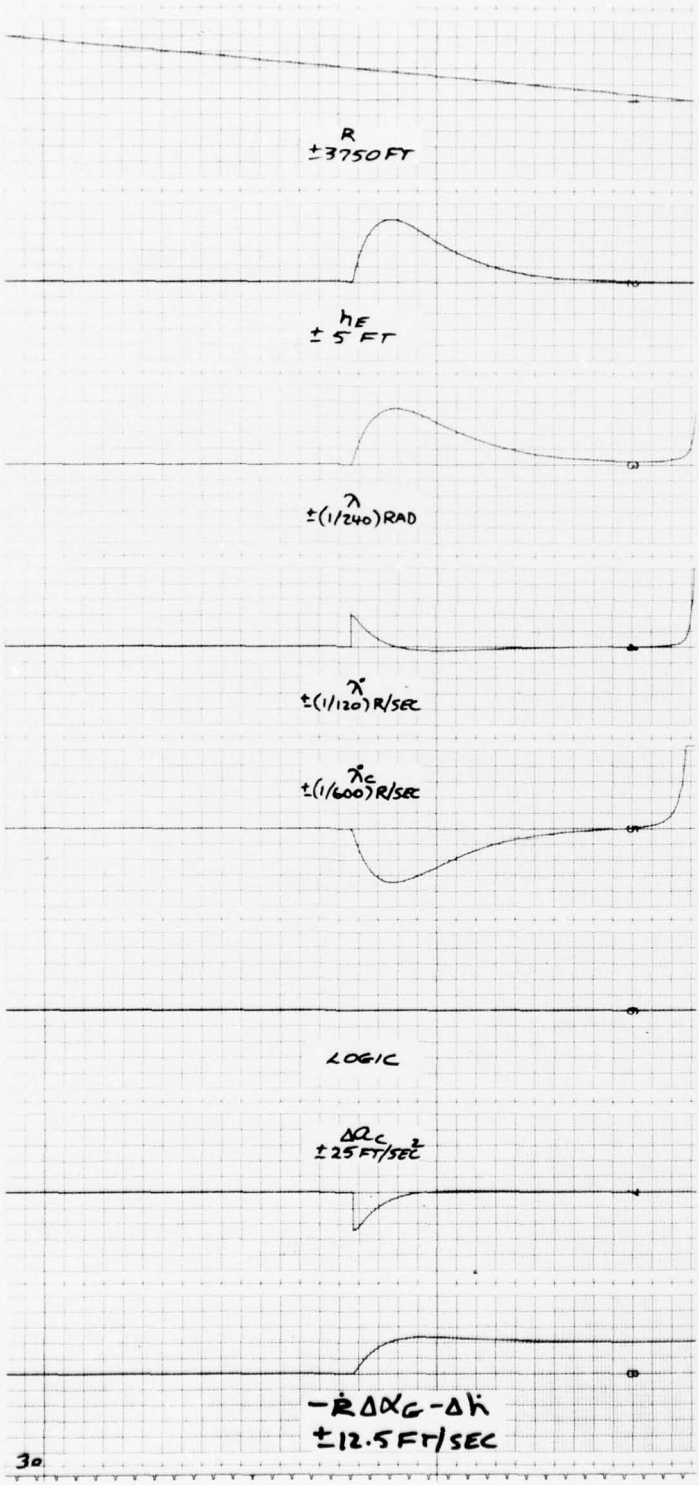

Figure 10. Ideal system gust response (ΔW_G = 5 ft/sec, R_m = 3000 ft, R_D = 1500 ft, n = 15)

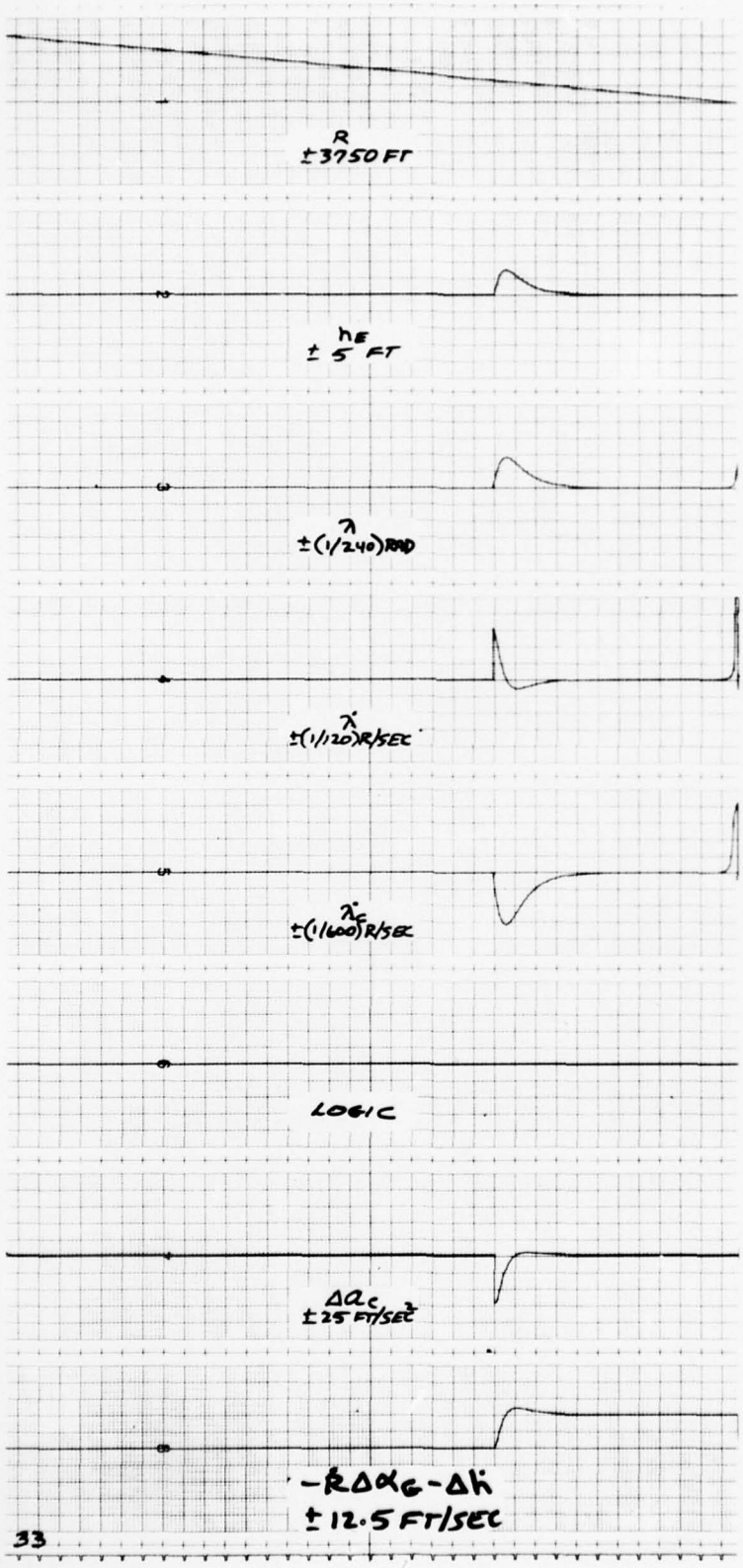

Figure 11. Ideal system gust response (ΔW_G = 5 ft/sec, R_m = 1000 ft, R_D = 1000 ft, n = 15)

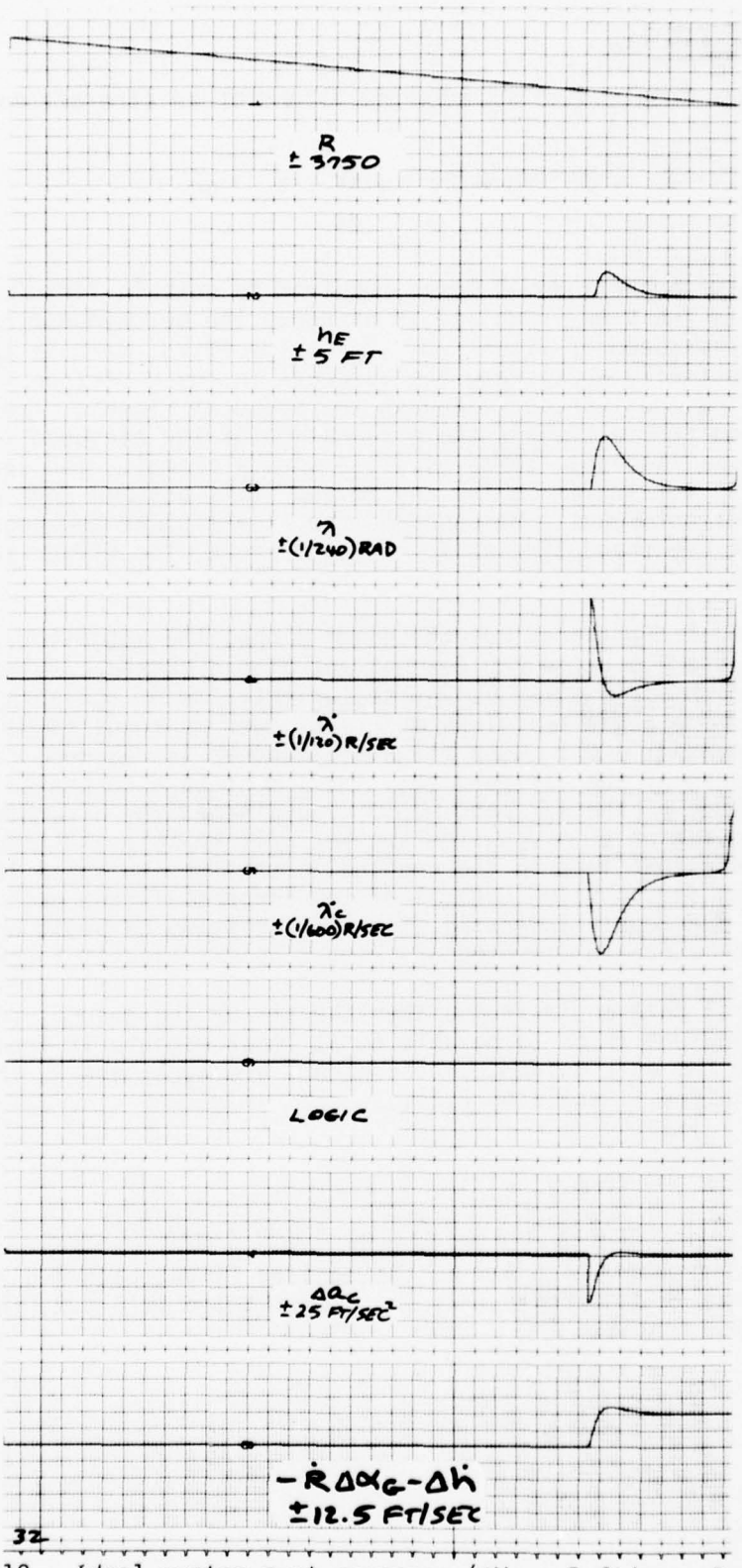

Figure 12. Ideal system gust response (ΔW_G = 5 ft/sec, R_m = 1000 ft, R_D = 600 ft, n = 15)

4. PATH ANGLE CONTROL

The power required to sustain the flight of an aircraft may be represented by,

$$P_{REQ} = \bar{L} \cdot \bar{W}_i + \bar{D} \cdot \bar{V}_W + \bar{V}_W \cdot m \frac{d\bar{V}}{dt} + \bar{V}_W \cdot m\bar{g} \qquad (4.1)$$

The first term is the induced power required to sustain lift ($\bar{L} \cdot \bar{W}_i$). The second term is the power required to overcome the aerodynamic drag of the aircraft at the airspeed of flight ($\bar{D} \cdot \bar{V}_W$). The third term is the power required to inertially accelerate the aircraft in any direction ($\bar{V}_W \cdot m\, d\bar{V}/dt$) such as turning, pull-up, or changing the speed of flight. The last term is the power required to sustain the orientation of the airspeed ($\bar{V}_W \cdot m\bar{g}$) relative to the gravitational force (e.g., a steady climb). The source of the power input to the system is the engine and it is assumed $P_{REQ} = P_{ENG}$ (i.e., the engine instantaneously responds to the flight power demands). The minimum value for the righthand side of 4.1 is, therefore, the flight idle power output of the engine.

When the aircraft acquires the glide slope, the autopilot is able to pitch the aircraft over to begin the descent and also decrease P_{ENG} to maintain the desired approach airspeed ($\bar{V}_W$). As the orientation of the airspeed ($\bar{V}_W$) steepens ($\bar{V}_W \cdot m\bar{g}$ more negative), less and less power is required to maintain airspeed ($\bar{V}_W \cdot m\, d\bar{V}/dt \equiv 0$). When flight idle power is reached, further increases in the steepness of the airspeed ($\bar{V}_W \cdot m\bar{g}$), must be accompanied by an increase in the magnitude of the airspeed ($\bar{V}_W$). The cleaner the aircraft is in the approach configuration ($\bar{D} \cdot \bar{V}_W$), the smaller will be this limiting path angle. These considerations lead to the conclusion that the guidance law must incorporate a means for positive control of the aircraft flight path angle (γ) in a descent. As previously indicated, this is necessary to avoid undesirable increases in the approach airspeed which must be arrested at touchdown.

To control path angle from either the air or the ground, one must be able to directly measure it or to be able to at least compute it from other measurements. Since the only guidance measurements are λ, $\dot{\lambda}$, and R, the latter approach is required. Recalling 2.25,

$$\dot{\lambda} = \dot{R} \frac{d\lambda}{dR} = \frac{-\dot{R}}{R} (\gamma + \gamma_F + \lambda) \qquad (4.2)$$

The only unknown quantity in 4.2 is the desired flight path angle (γ). If the desired maximum descent angle ($-\gamma_L$) is substituted into 4.2, then a limit on the allowable $\dot{\lambda}$ results.

$$\dot{\lambda}_{\overline{CLIM}} = -\frac{\dot{R}}{R} (-\gamma_L + \gamma_F + \lambda) \qquad (4.3)$$

The intent is to subject 3.12 and 3.13 to a command limiting process as defined by 4.3. The command limit ($\dot{\lambda}_{CLIM}$) is variable being a function of instantaneous range and angular error. In addition to functioning as a command limit, $\dot{\lambda}_{CLIM}$ can also act as an automatic abort signal. Normally $\dot{\lambda}_{CLIM}$ is negative as γ_L is certainly greater than γ_E and $\dot{\lambda}$ is nominally zero. A positive value for $\dot{\lambda}_{CLIM}$ indicates that λ has become, either at acquisition or later in the approach, too large to execute the maneuvers to touchdown. This would be even more important if a positive limit $\dot{\lambda}^{+}_{CLIM}$ was imposed on the guidance law to avoid attempting to climb at too steep an angle for the maximum engine power available. The positive limit will not be considered further here as a complete engine simulation is necessary to explore this boundary of the flight envelope.

The complete guidance law is,

$$a_C = (-2\dot{R})(n+2)\left(\frac{R}{R'}\right)(\dot{\lambda}'_C - \dot{\lambda}) \tag{4.4}$$

where,

$$\dot{\lambda}_C = -\dot{R}\left[\frac{-}{1} - \left(\frac{n+3}{2}\right)\left(\frac{R}{R'}\right)\right](\lambda/R) \tag{4.5}$$

and,

$$\left.\begin{aligned} \dot{\lambda}'_C &= \dot{\lambda}_C \quad \text{if } \dot{\lambda}_C \leq \dot{\lambda}^{-}_{CLIM} \\ \dot{\lambda}'_C &= \dot{\lambda}^{-}_{CLIM} \quad \text{if } \dot{\lambda}_C \geq \dot{\lambda}^{-}_{CLIM} \end{aligned}\right\} \tag{4.6}$$

and,

$$\left.\begin{aligned} R' &= R \quad \text{if } R \geq R_m \\ R' &= R_m \quad \text{if } R \leq R_m \end{aligned}\right\} \tag{4.7}$$

Figure 13 depicts the ideal system response ($\Delta a = \Delta a_C$) for the guidance law (4.4) from acquisition at R = 3000 feet and Δh_E = 100 feet to touchdown. The channel labeled "LOGIC" indicated the fraction of the flight path during which command limiting of $\dot{\lambda}$ was in effect ($\gamma_L = 8^{o}$).

5. AIRFRAME/AUTOPILOT REPRESENTATION

There is a tendency to consider the complete airborne computing capability (analog or digital considerations are of no consequence) as the "auto-pilot." Under such circumstances, the design objectives of the guidance function and the control function may become unnecessarily interrelated or even obscured. The view taken within this report is that the control function pertains to the control of forces, of any origin, which act on the aircraft. The aerodynamic and inertial forces on the aircraft are predominately a function of the translational (U, V, W) and rotational (p, q, r) rates of the airframe and their

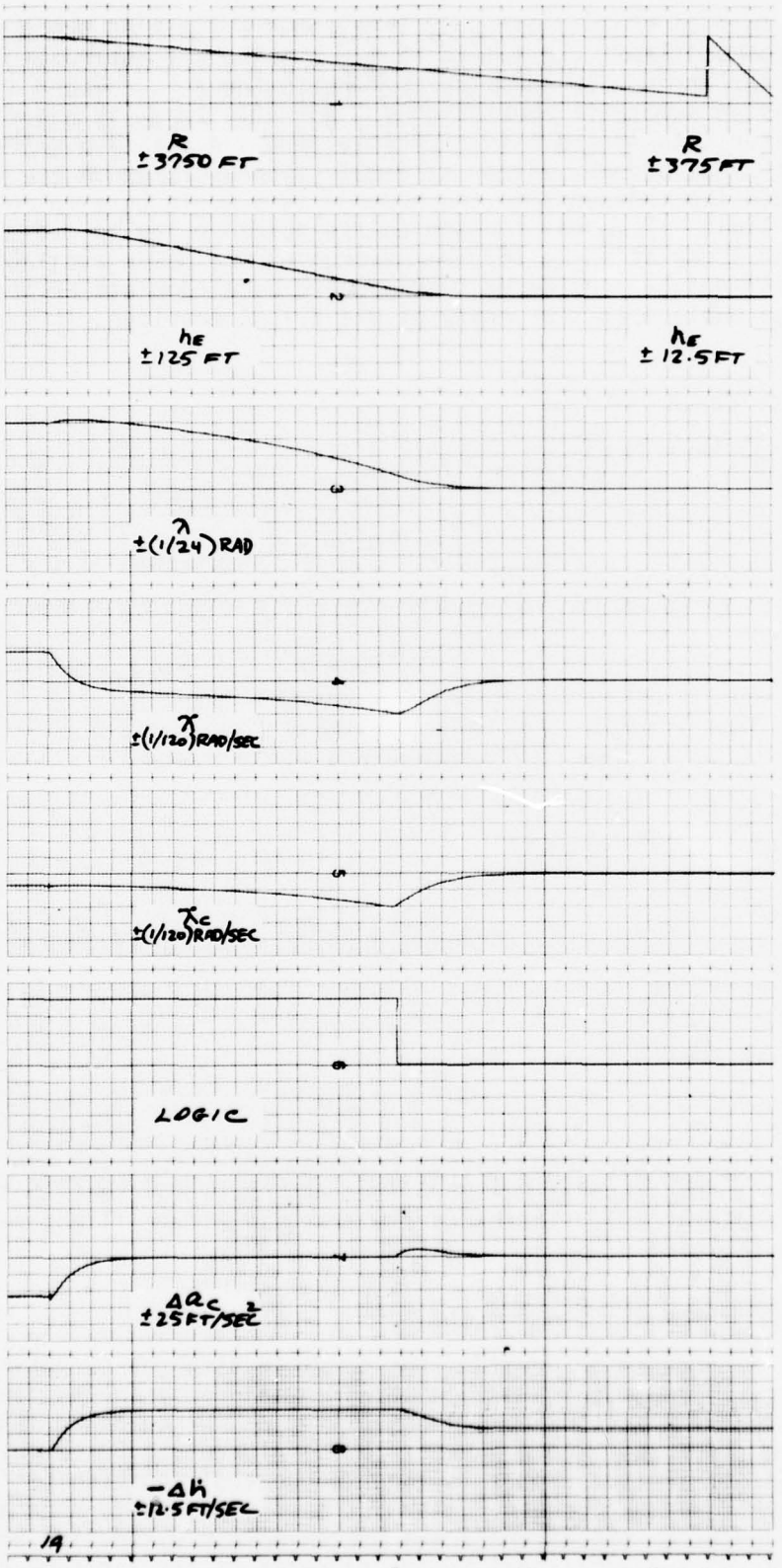

Figure 13. Ideal system response ($\gamma_L = 8^0$, $\gamma_F = 4^0$, R_m = 1000 ft, n = 15, $\dot{R}$ = -85 ft/sec)

derivatives, while the gravitational force is a function of the angular orientation (ϕ, θ) of the airframe. Within this framework, control of airspeed, altitude rate, glide path angle, pitch and roll attitude, and normal acceleration are all considered autopilot functions, while control of heading (ψ), altitude (h), translational position (N, E) or even the λ, $\dot{\lambda}$ variables of this document are all considered guidance functions.

The pertinent quantities for autopilot control in this document are primarily the normal acceleration and secondarily, the airspeed. The design objectives for the autopilot are:

a. To stabilize the short period and phugoid modes of airframe motion.

b. To minimize the variability in normal acceleration response per unit of command input.

c. To minimize the change in flight path angle (γ) produced by a vertical wind gust.

The goal of this section is the synthesis of an autopilot concept rather than an autopilot design. No attempt is made to optimize the parameters within the concept to best satisfy the above objectives. Emphasis is placed upon qualitatively showing how each parameter impacts the various objectives and upon arriving at a conservative design framework for later optimization. The technical approach used herein relies heavily upon analog-computer simulation as a design tool. Analysis is used to explain the results of the simulation.

The simulation of this report utilizes a linearization of the airframe dynamics about a nominal condition of straight and level flight at the desired approach airspeed. The stability derivatives are estimates of a typical flying wing RPV configuration. The specific characteristics of the engine have been neglected for this effort and only the response of the airframe to a perturbation in thrust ($\Delta T/m$) is considered. While perturbation aerodynamics are used throughout, most kinematic relationships were retained in their nonlinear form. The coordinate system used herein is of the body fixed variety with its origin at the center of mass of the airframe. The linear accelerations along the rotating X axis ($\dot{U}$) and Z axis ($\dot{W}$), and the angular accelerations about the Y axis ($\ddot{\theta}$) are;

$$\dot{\Delta U} = X_W \, \Delta W_A + X_u \, \Delta U - g \, \Delta\theta + \Delta T/m \tag{5.1}$$

$$\dot{\Delta W} = U \, \dot{\Delta\theta} - \dot{\Delta a} = U \, (\dot{\Delta\theta} - \dot{\Delta\gamma}) \tag{5.2}$$

$$\ddot{\Delta\theta} = M_\theta \, \dot{\Delta\theta} + M_W \, \Delta W_a + M_\delta \, \Delta\delta_E \tag{5.3}$$

where

$$\Delta a = - Z_\delta \, \Delta\delta_E - Z_W \, \Delta W_a - Z_u \, \Delta U \tag{5.4}$$

$$\Delta W_A = \Delta W + \Delta W_G \tag{5.5}$$

$$U = U_0 + \Delta U \tag{5.6}$$

The quantity Δa is the perturbation normal acceleration of the center of mass. A normal accelerometer mounted a distance ℓ_T in front of the airframe center of mass will sense.

$$\Delta a_m = \Delta a + \ell_T \ddot{\Delta\theta} \tag{5.7}$$

The guidance law functions in a closed-loop fashion on the angular error (λ) hence from (2.25),

$$\dot{\lambda} = \frac{U}{R} [\gamma + \gamma_F + \lambda)] \tag{5.8}$$

or

$$\dot{\lambda} = \frac{-1}{R} [- \Delta W + U (\Delta\theta + \gamma_F + \lambda)] \tag{5.9}$$

and

$$\lambda = \int_0^t \dot{\lambda}\, dt + \lambda_0 \tag{5.10}$$

The altitude error at any range is found from the <u>open-loop</u> calculation

$$h_E = R\, \lambda \tag{5.11}$$

so that one must be especially cautious of scaling difficulties (e.g., λ and R are both approaching zero). The simulation results within this document may be suspect for perhaps the last 2 seconds of flight (170 feet) due to analog scaling difficulties with λ and R. This is purely a simulation difficulty and, in any event, determination of absolute errors at recovery is not the intent of this effort.

The following stability derivatives were used in the simulation:

$$\begin{aligned}
X_w &= .2 \ (\text{Sec}^{-1}) \\
X_u &= -.1 \ (\text{Sec}^{-1}) \\
Z_w &= -3. \ (\text{Sec}^{-1}) \\
Z_u &= -.75 \ (\text{Sec}^{-1}) \\
Z_\delta &= -50. \ (\text{Ft} - \text{Sec}^{-2}) \\
M_w &= -.1 \ (\text{Ft}^{-1} - \text{Sec}^{-1}) \\
M_{\dot{\theta}} &= -.6 \ (\text{Sec}^{-1}) \\
M_\delta &= -20. \ (\text{Sec}^{-2}) \\
U_0 &= 85. \ (\text{Ft} - \text{Sec}^{-1})
\end{aligned} \tag{5.12}$$

Appendix A contains the scaled analog computer simulation diagrams for equations (5.1) through (5.11).

The set of equations (4.4 through 4.7) relate how the normal acceleration (Δa) should vary as a function of the range (R), the angular error (λ) relative to the desired straight line approach path of slope (γ_F), and the approach ground speed ($-\dot{R}$). The set of equations (5.1 through 5.6) relate how the normal acceleration (Δa) varies as a function of the aircraft input state ($\Delta T/m$, $\Delta\delta_E$, ΔW_G). The function of the autopilot is to manipulate ΔT and $\Delta\delta_E$ to cause Δa to follow the desired command (Δa_C) in the presence of disturbances (ΔW_G) and at the desired speed of approach ($-\dot{R}$). The landing technique most familiar to all is to manipulate the elevons ($\Delta\delta_E$) to control descent attitude and hence the speed of approach, and to manipulate the throttle to control rate of climb ($\Delta\dot{h}$). While this technique is safe in that it avoids attempting to climb at an excessive rate (e.g., no worse than a full throttle, constant airspeed climb), it is usually unacceptable for precise approaches due to the sluggishness of the response of climb rate to a throttle input. This sluggishness impacts both the control response (e.g., how fast can a commanded ascent/descent rate be established?) as well as the gust response (e.g., how fast can a gust-induced error rate be arrested?). The more responsive technique is to manipulate the throttle (ΔT) to control airspeed and to manipulate the elevons ($\Delta\delta_E$) to control rate of climb or more precisely normal acceleration. One must be cautious in using this technique as it is possible to transiently establish a climb rate which cannot be sustained due to insufficient power available. Additionally, if the aircraft is trimmed on the backside of the drag curve, the maneuver is not very stable (i.e., an increase in angle of attack increases the drag more than the lift.)

The behavior of normal acceleration control by elevon manipulation will be investigated by consideration of an approximate set of differential equations for which Δu is assumed zero. A physical view of this assumption is that the throttle is being deftly manipulated to hold Δu identically equal to zero regardless of variations in $\Delta\theta$, Δw, and Δa.

From 5.1 through 5.6,

$$\begin{bmatrix} S & -U_o\,S & 1 \\ -M_w & S(S - M_{\dot{\theta}}) & 0 \\ Z_w & 0 & 1 \end{bmatrix} \begin{bmatrix} \Delta w \\ \Delta\theta \\ \Delta a \end{bmatrix} = \begin{bmatrix} 0 \\ M_\delta \\ -Z_\delta \end{bmatrix} \Delta\delta_E \qquad (5.13)$$

One may compute the transfer function relating normal acceleration to elevon deflection as,

$$\frac{\Delta a}{\Delta\delta_E} = \frac{-Z_\delta\,S^2 + Z_\delta\,M_{\dot{\theta}}\,S + U_o\,(Z_\delta\,M_w - M_\delta\,Z_w)}{(S - M_{\dot{\theta}})\,(S - Z_w) - U_o\,M_w} \qquad (5.14)$$

Using the stability derivatives (5.12) one may assume,

$$Z_\delta\,M_w \ll M_\delta\,Z_w \qquad (5.15)$$

and also

$$\frac{\Delta a}{\Delta \delta_E} = \frac{- Z_\delta S^2 + Z_\delta M_{\dot{\theta}} S - M_\delta Z_w U_o}{(S - M_{\dot{\theta}})(S - Z_w) - U_o M_w} \tag{5.16}$$

The denominator is the most fundamental approximation to the short period mode of aircraft motion. The steady state relationship between Δa and $\Delta \delta_E$ is approximately,

$$\frac{\Delta a}{\Delta \delta_E} = \left(\frac{M_\delta}{M_w}\right) Z_w \tag{5.17}$$

As indicated, one of the main functions of the autopilot is to reduce the variability in how much acceleration is produced by a unit of command input. (NOTE: Only for the case of no feedback does one unit of command input correspond to one unit of elevon deflection.) The above relationship (5.17) implicitly indicates the primary source of this variability, being the change in M_w produced by variations in the location of the aircraft center of mass. Figure 14 depicts the behavior of the approximate equations (5.13) in response to an elevon input, for two values of M_w. The use of feedback to reduce this variability is fundamental. The quantity to be used as the feedback signal is, of course, the normal acceleration itself.

In addition to reducing the variability of the normal acceleration response, the use of an acceleration feedback causes a more oscillatory short period mode. Assume for now that one may neglect the effects of elevon lift (Z_δ) in (5.13) and,

$$\Delta \delta_E = K_a (\Delta a_c - \Delta a) \tag{5.18}$$

Combining (5.13) and (5.18) one finds,

$$\frac{\Delta a}{\Delta a_c} = \frac{-U_o M_\delta Z_w K_a}{(S - M_{\dot{\theta}})(S - Z_w) - U_o (M_w + M_\delta Z_w K_a)} \tag{5.19}$$

Examination of the denominator of (5.19) shows that the K_a feedback has the same effect on the short period mode as does the "aerodynamic spring" or static stability derivative (M_w). Increases in the gain of the normal acceleration feedback will eventually have to be dampened by a pitch rate feedback. The appearance of the K_a term in the numerator is due to the acceleration error ($\Delta a_c - \Delta a$) formulation of (5.18). This is, of course, fundamental to achieving the desired relatively invarient acceleration response. In the steady state,

$$\frac{\Delta a}{\Delta a_c} = \frac{- U_o M_\delta Z_w K_a}{M_{\dot{\theta}} Z_w - U_o M_w - U_o M_\delta Z_w K_a} \tag{5.20}$$

For large K_a, variations in M_w have the desired negligible effect on the Δa response per unit of command input (Δa_c). Using $K_a = .007$ radians per feet per second^2, expression (5.20) becomes,

$$\frac{\Delta a}{\Delta a_c} = \frac{36}{1.8 + 8.5 + 36} = .78 \tag{5.21}$$

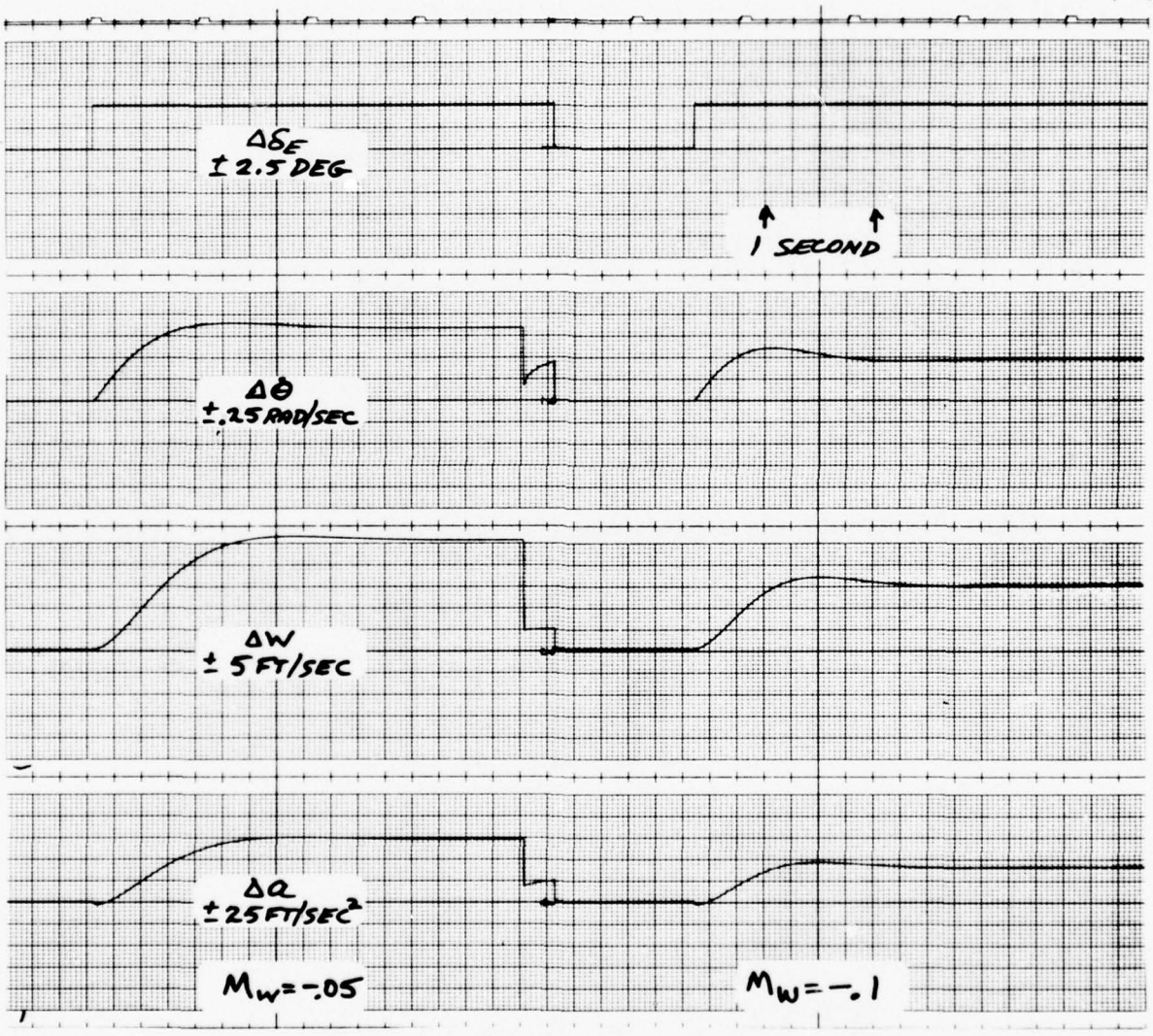

Figure 14. Short period response ($\Delta l' = 0$) to a step elevon input

Figure 15 demonstrates (1) the relative invariance of the Δa response for two values of M_w(2), the roughly 20 percent difference between the commanded acceleration (Δa_c) and the normal acceleration (Δa), and (3) the more oscillatory short period mode caused by the acceleration feedback increasing the short period frequency of oscillation (W_{SP} = 6.8 rad/sec versus the unaugmented W_{SP} = 3.2 rad/sec). The value of Δa_c in Figure 15 was chosen to produce the same initial elevon deflection as in Figure 14 ($\Delta\delta_E$ = 1 degree). The decreased steady state acceleration achieved in Figure 15 is the result of the feedback signal dynamically decreasing the elevon input from its initial value.

The feedback actually used in Figure 15 was not the acceleration of the center of mass (Δa), but rather the acceleration (Δa_m) of a point ℓ_T feet in front of the center of mass. The initial jump in Δa is due to a lift upon the elevons (Z_δ), neglected in the above treatment. The sense of this force is opposite to the eventual steady state and is hence detrimental to the stability of a Δa to $\Delta\delta_E$ control system. Location of the sensing accelerometer at the instantaneous center of rotation ($\ell_T = M_\delta/Z_\delta$ = 2.5 feet) negates the detrimental effect. Note in Figure 15 that the feedback signal Δa_m is initially zero for ℓ_T = 2.5 feet. For the same command input (ΔA_C), Figure 16 shows the amplification of the elevon lift effect by feedback of the acceleration of the center of mass ($\Delta a_m = \Delta a$). For sufficient gain (K_a), the nonminumum phase behavior of this feedback ($\Delta a_m = \Delta a$) would lead to a static instability of the short period mode. For all remaining simulation traces in this report, the sensing accelerometer is located at the instantaneous center of rotation.

Figure 17 depicts the approximate short period response with both a normal acceleration (Δa_m) and a pitch rate ($\Delta\theta$) feedback. Using,

$$\begin{bmatrix} S & -U_o S & 1 \\ -M_w & S\,(S - M_{\dot\theta}) & 0 \\ Z_w & 0 & 1 \end{bmatrix} \begin{bmatrix} \Delta W \\ \Delta\theta \\ \Delta a_m \end{bmatrix} = \begin{bmatrix} 0 \\ M_\delta \\ 0 \end{bmatrix} \Delta\delta_E \qquad (5.22)$$

and,

$$\Delta\delta_E = K_a\,(\Delta a_c - \Delta a_m) - K_{\dot\theta}\,\dot{\Delta\theta} \qquad (5.23)$$

one finds,

$$\frac{\Delta a_m}{\Delta a_c} = \frac{-U_o M_\delta Z_w K_a}{(S - M_{\dot\theta} + K_{\dot\theta} M_\delta)(S - Z_w) - U_o (M_w + M_\delta K_a Z_w)} \qquad (5.24)$$

Not only does the pitch rate feedback act to dampen the more oscillatory short period mode, but it also increases the steady state error between Δa_m and Δa_c. Consider the steady state of 5.24

$$\frac{\Delta a_m}{\Delta a_c} = \frac{-U_o M_\delta Z_w K_a}{Z_w (M_{\dot\theta} - K_{\dot\theta} M_\delta) - U_o (M_w + M_\delta K_a Z_w)} \qquad (5.25)$$

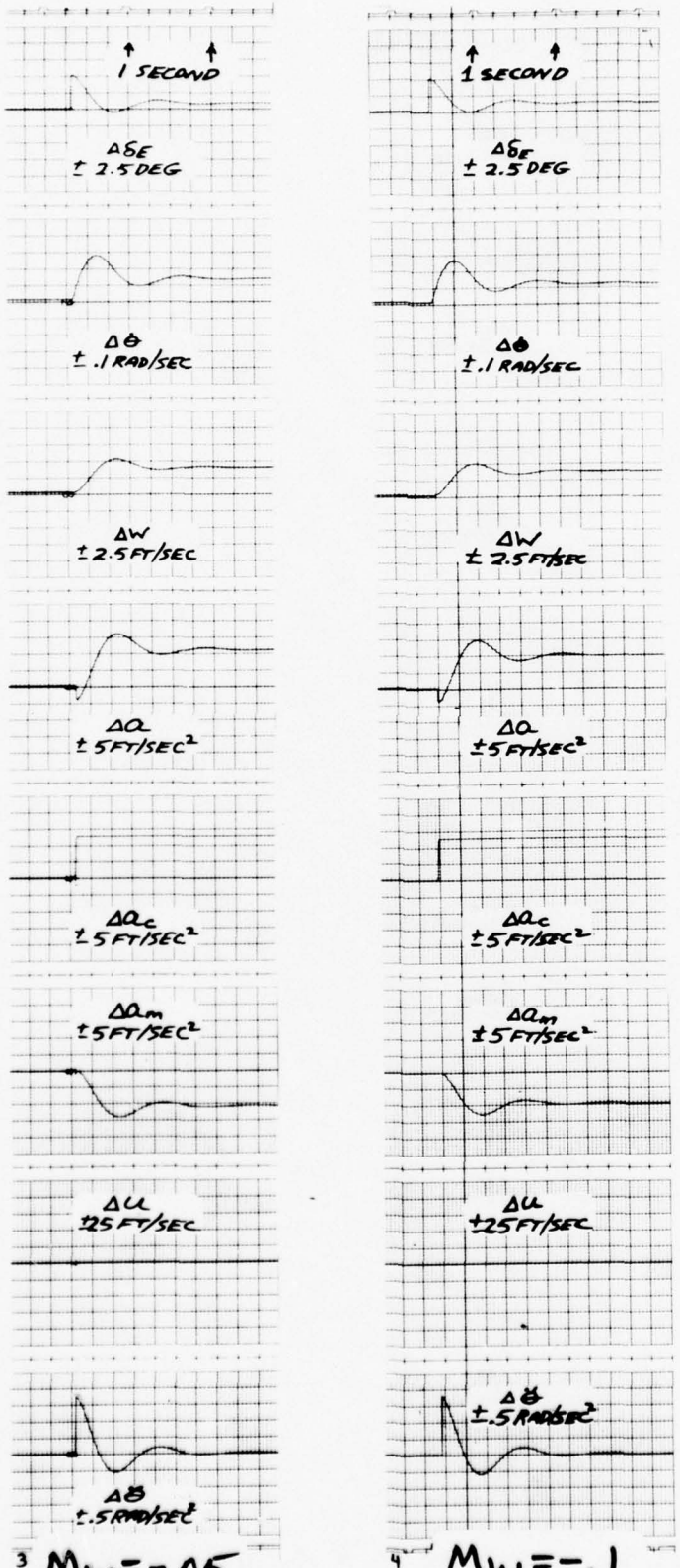

Figure 15. Short period response (K_a = -0.007) to a step command input (Δa_c)

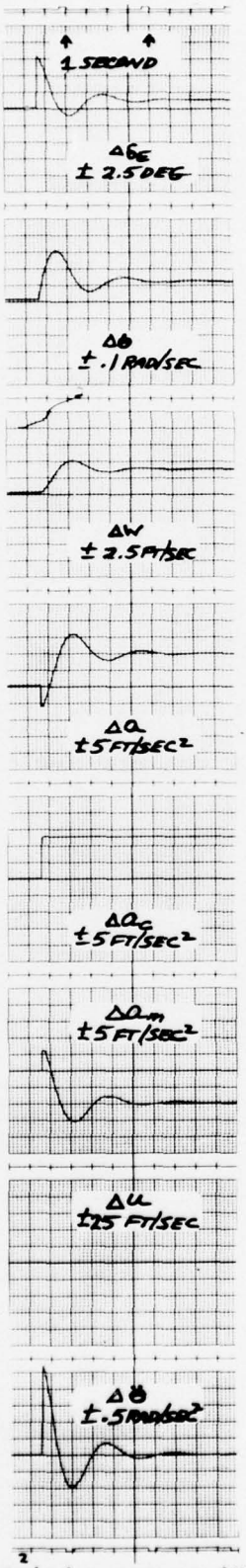

Figure 16. Short period response (K_a = -0.007) to a Δa_c step with δ_T = 0

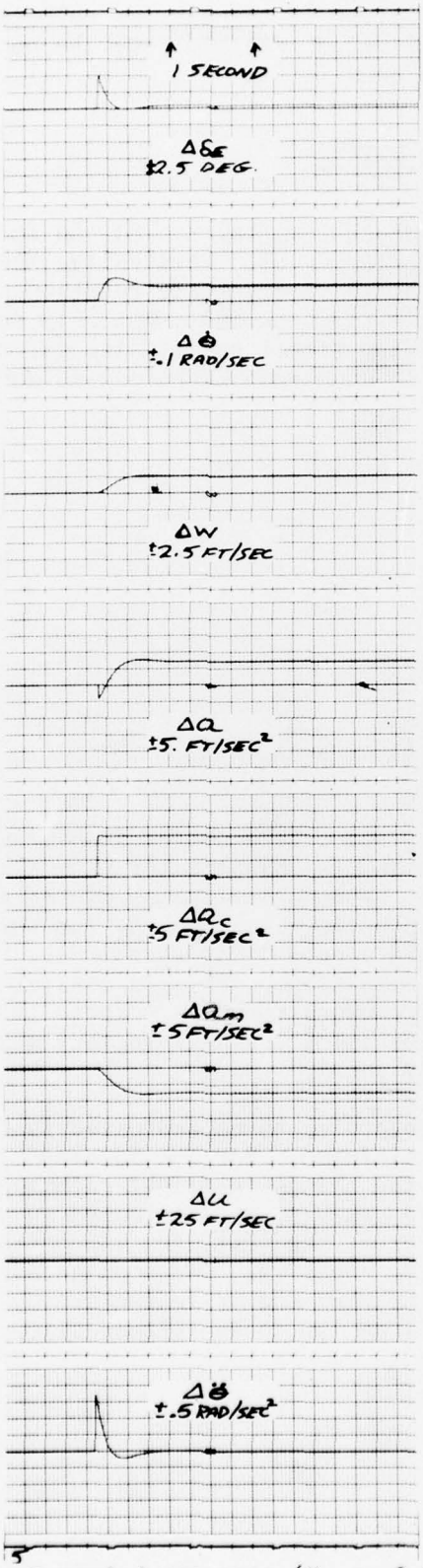

Figure 17. Short period response (K_a = -0.007, $K_{\dot{\theta}}$ = -0.35) to a Δa_c step

Using the stability derivatives (5.12) and the selected feedback gains (Ka = - .007 rad/ft/sec^2 and $K_{\dot{\theta}}$ = - .35 rad/rad/sec) the numerical factors of the steady state relationship are,

$$\frac{\Delta a_m}{\Delta a_c} = \frac{36.}{1.8 + 21. + 8.5 + 36} = .53 \tag{5.26}$$

For pure acceleration feedback ($\Delta a_m/\Delta a_c$ = .78) and for pitch rate dampened acceleration feedback, $\Delta a_m/\Delta a_c$ = .53. Physically, the additional error is developed because a prescribed steady state relationship exists between normal acceleration and pitch rate ($\Delta a = u_o \Delta\dot{\theta}$). Not only does the pitch rate contribute a transient dampening effect but it also introduces predictable steady state effects. This can be countered by a feed-forward path in the autopilot (Figure 18) from which,

$$\Delta\delta_E = K_a (\Delta a_c - \Delta a) + K_{\dot{\theta}} (\Delta\dot{\theta}_c - \Delta\dot{\theta}) \tag{5.27}$$

where

$$\Delta\dot{\theta}_c = \frac{\Delta a_c}{U_o} \tag{5.28}$$

Equations (5.27) and (5.28) may be combined to obtain,

$$\Delta\delta_E = K_a \left[\left(1 + \frac{K_{\dot{\theta}}}{K_a U_o}\right)\Delta a_c - \Delta a\right] - K_{\dot{\theta}} \Delta\dot{\theta} \tag{5.29}$$

The feed-forward path does not affect system stability and is equivalent to multiplying the input command Δa_c by a factor ($1 + K_{\dot{\theta}}/K_a U_o$). For the chosen gains and approach speed, the numerical value of the factor is 1.59. The overall idealized relationship between Δa_m and Δa_c for the pitch-rate-dampened, acceleration feedback would become ($\Delta a_m/\Delta a_c$ = .85). The feed-forward feature was not included in this simulation. This is consistent with the intent to maintain a conservative framework for this effort. If the performance of the coupled guidance/control dynamics are satisfactory with $\Delta a_m \sim .5\Delta a_c$ then the design concept is relatively sound.

The next autopilot objective to be addressed is the wind gust (ΔW_G) response of the stabilized airframe. For the landing mission, the gust characteristics of interest is the change in flight path angle (γ) produced by the angle of attack gust ($\alpha_G = \Delta W_G/U_o$). As indicated in section 3, if attitude is maintained ($\Delta\theta = 0$) during the gust, the change in $\Delta\gamma$ is precisely $\Delta\alpha_G$. For a statically stable (M_w negative), unaugmented airframe, the natural tendency is to rotate into the wind and drive the steady state angle of attack ($\Delta\alpha_A = \Delta W_A/U_o$) to zero. That is, in the steady state,

$$\Delta\theta = \Delta\gamma - \Delta\alpha_G \tag{5.30}$$

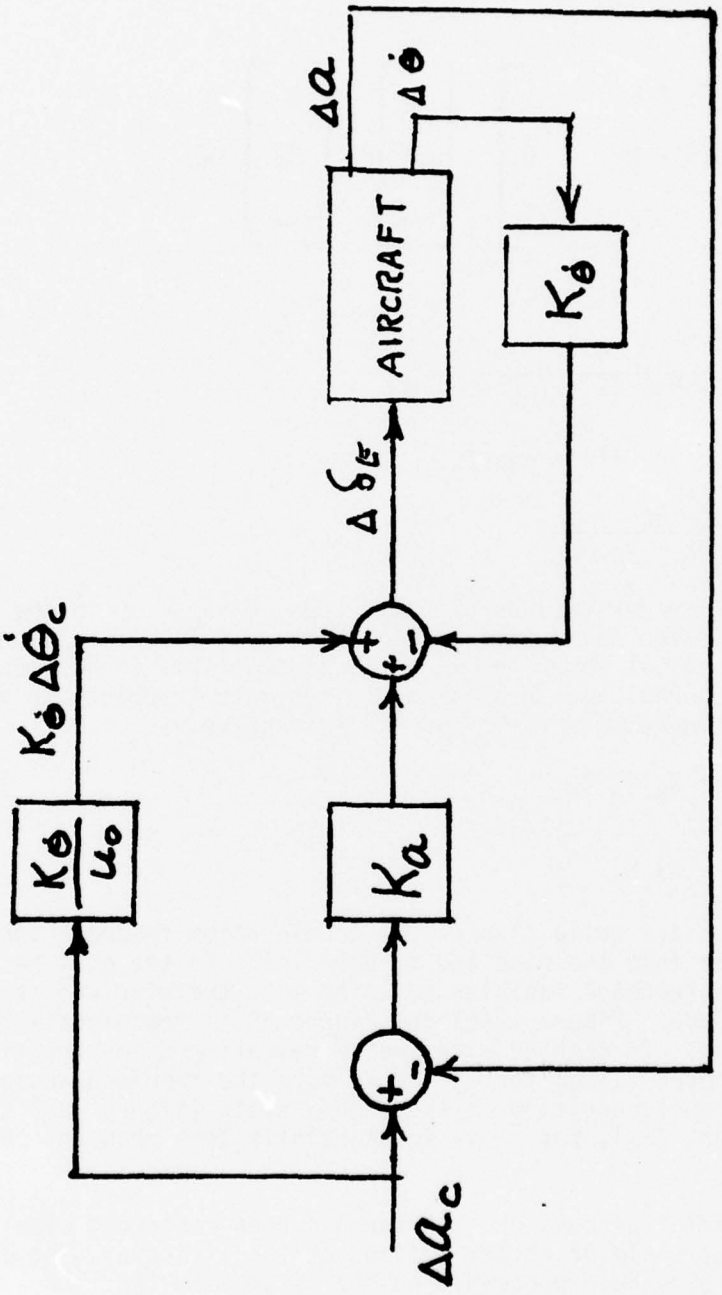

Figure 18. Acceleration autopilot with feed forward path

or

$$\frac{\Delta\gamma}{\Delta\alpha_G} = 1 + \frac{\Delta\theta}{\Delta\alpha_G} \tag{5.31}$$

From

$$\begin{bmatrix} S & -U_o\, S & 1 \\ -M_w & S(S - M_{\dot\theta}) & 0 \\ Z_w & 0 & 1 \end{bmatrix} \begin{bmatrix} \Delta W \\ \Delta\theta \\ \Delta a_m \end{bmatrix} = \begin{bmatrix} 0 \\ M_w \\ -Z_w \end{bmatrix} \Delta W_G \tag{5.32}$$

then

$$\frac{\Delta\theta}{\Delta\alpha_G} = \frac{M_w\, U_o}{(S - M_{\dot\theta})\,(S - Z_w) - U_o\, M_w} \tag{5.33}$$

which in the steady state equals,

$$\frac{\Delta\theta}{\Delta\alpha_G} = \frac{M_w\, U_o}{Z_w\, M_{\dot\theta} - U_o\, M_w} \tag{5.34}$$

For the stability derivatives of 5.12, then $\Delta\theta/\Delta\alpha_G = .9$ in the steady state. The response of the basic airframe to a downgust ($\Delta\alpha_G = -3.4$ degrees or $\Delta W_G = -5$ ft/sec) is shown in Figure 19a and confirms expression (5.34). As seen earlier, normal acceleration and pitch rate feedbacks to the elevons may be treated as increments to M_w and $M_{\dot\theta}$, respectively.

$$\begin{aligned} M_w' &= M_w + K_a\, M_\delta\, Z_w \\ M_{\dot\theta}' &= M_{\dot\theta} - K_{\dot\theta}\, M_\delta \end{aligned} \tag{5.35}$$

The conclusions are quite clear. The acceleration feedback increases the tendency to rotate into the wind and is beneficial to the gust response, while the pitch rate feedback inhibits rotation into the wind and is detrimental to the gust response. Figure 19(b) and Figure 20(a) demonstrate these individual characteristics. In keeping with the aforementioned conservative design approach, the chosen values for K_a and $K_{\dot\theta}$ make the combined augmented system somewhat more gust sensitive in the steady state (Figure 20b) than the basic airframe (Figure 19a), but still substantially less than the $\Delta\theta = 0$ analysis of section 3.

The autopilot discussion thus far has been concerned with control of the short period or angle of attack motions of the airframe. The discussion and simulation results have proceeded on the assumption that thrust variations of the engine maintain ΔU identically equal to zero. In a similar fashion, phugoid airframe motions can be visualized by the assumption of $\Delta W = 0$. This is equivalent to the airframe having a quick stable short period mode so that angle of attack motions may be neglected. The phugoid mode is dominated by variations in the X and Z forces due to ΔU and $\Delta\theta$ perturbations.

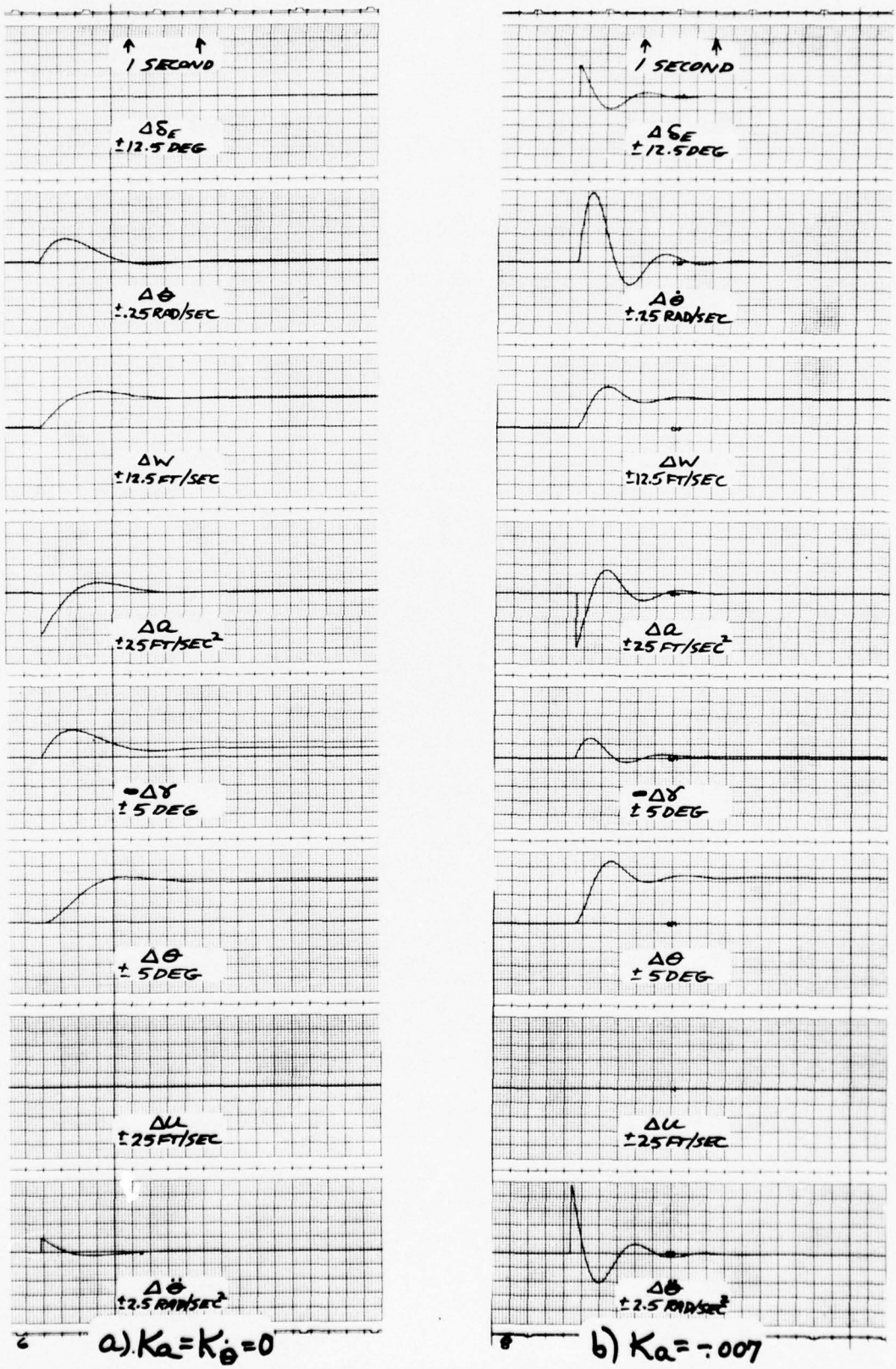

Figure 19. Short period gust response (ΔW_G = -0.5 ft/sec)

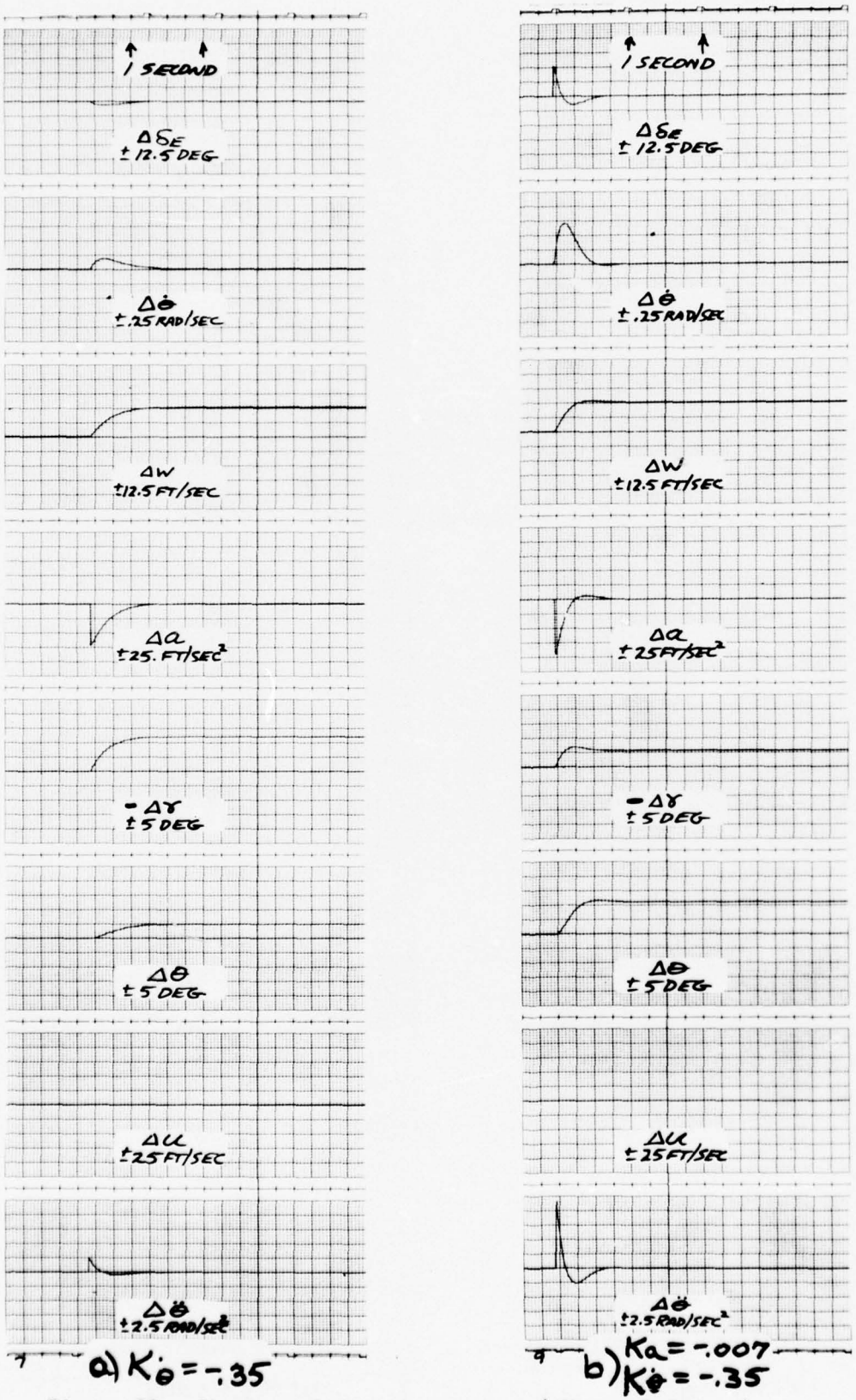

Figure 20. Short period gust response (ΔW_G = =5 ft/sec)

$$\begin{bmatrix} S - X_u & g \\ Z_u & S\,U_o \end{bmatrix} \begin{bmatrix} \Delta U \\ \Delta\theta \end{bmatrix} = 0 \qquad (5.36)$$

or

$$S^2 - X_u S - \frac{Z_u\, g}{U_o} = 0 \qquad (5.37)$$

The lightly dampened approximation to the phugoid mode is shown in Figure 21. The $\Delta W = 0$ constraint was approximated on the simulation trace by increasing M_w (- 1. versus -.1). The most direct method of damping the phugoid is to increase the drag of the airframe. Modulation of the thrust of the engine is equivalent but too small in magnitude to be useful. Deployment of drag brakes would permit steeper descents as well as dampen the phugoid but this approach is not considered here. The usual means of increasing phugoid damping is to feed low frequency pitch attitude information back to the elevons. (Gust response considerations preclude high frequency pitch attitude feedback). Because the RPV mission tends to require extended periods of circling, a vertical gyro is not usually part of the RPV sensor package and low frequency filtering of pitch rate to obtain quasi-attitude information is undesirable because of the filter initialization difficulties which are typical of such implementations. The approach taken here, therefore, is to rely on the Δa, $\Delta\dot{\theta}$ autopilot feedbacks as well as the low frequency λ, $\dot{\lambda}$ guidance feedbacks to maintain control of the phugoid motions.

Figure 22 is a simulation trace of the complete airframe motions (5.1 to 5.12) in response to a 5 ft/sec wind gust (ΔW_G). The phugoid mode has less damping than the classical phugoid ($\Delta W = 0$) due to coupling of the ΔW motions ($M_w = - .1$) with the ΔU, $\Delta\theta$ motions. The period of the phugoid motion (W_p^{-1} = 13 seconds is relatively unaffected by the ΔW degree of freedom. The incorporation of a normal acceleration feedback affects both the short period and the phugoid modes of motion. As indicated in Figure 23, the damping of the phugoid mode is more like the classical phugoid case (Figure 21). The acceleration feedback has quickened the short period mode and made the $\Delta W = 0$ approximation of Figure 21 more valid than for the unaugmented airframe case of Figure 22. Another effect of the feedback is to convert the phugoid motions into lower frequency (W_p^{-1} = 28 seconds), slightly higher amplitude motions. This is beneficial as the lower frequency behavior is more amenable to stabilization by the guidance feedbacks (λ,$\dot{\lambda}$) on approach. A pure pitch rate feedback has the same low frequency effects upon phugoid stability as does the normal acceleration feedback (e.g., $\Delta a \simeq U_o\, \Delta\dot{\theta}$). An important difference, however, is the magnitude of the excitation of the phugoid motion. As can be seen in a comparison of Figures 23 and 24, the $\Delta\theta$ induced by the initial wind gust is much greater for the Δa feedback than for $\Delta\theta$ case. It is apparent that the price to be paid for the ΔW_G gust alleviation character of the Δa feedback, is increased excitation of the phugoid mode. The combined effects of the $\Delta\theta$ and Δa feedbacks are shown in Figure 25.

The coupled set of perturbation equations (5.1 through 5.6) together with the stability derivatives (5.12) are stable. As a result of being stable, when these equations are perturbed from their trim value by a step wind gust (ΔW_G), the aircraft will eventually return to this trimmed aerodynamic state

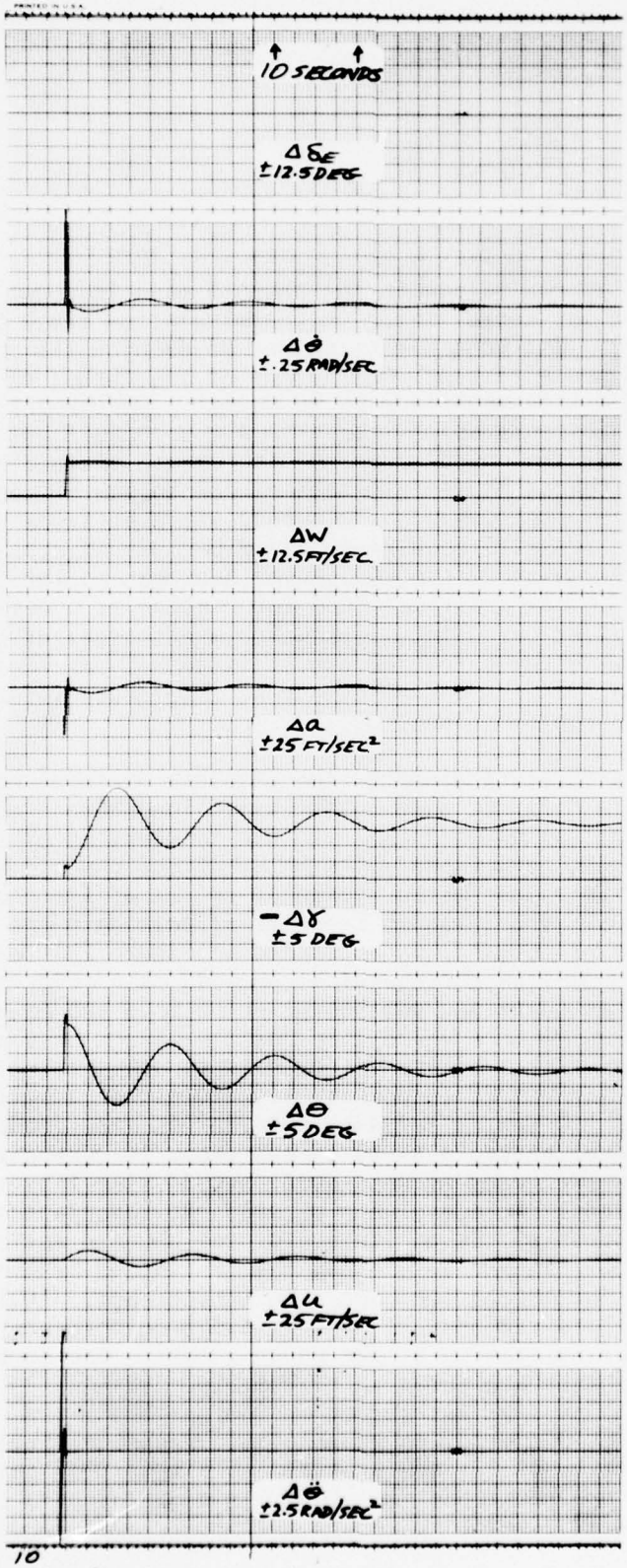

Figure 21. Classical phugoid ($\Delta W = 0$) response to a gust input (ΔW_G = -5 ft/sec)

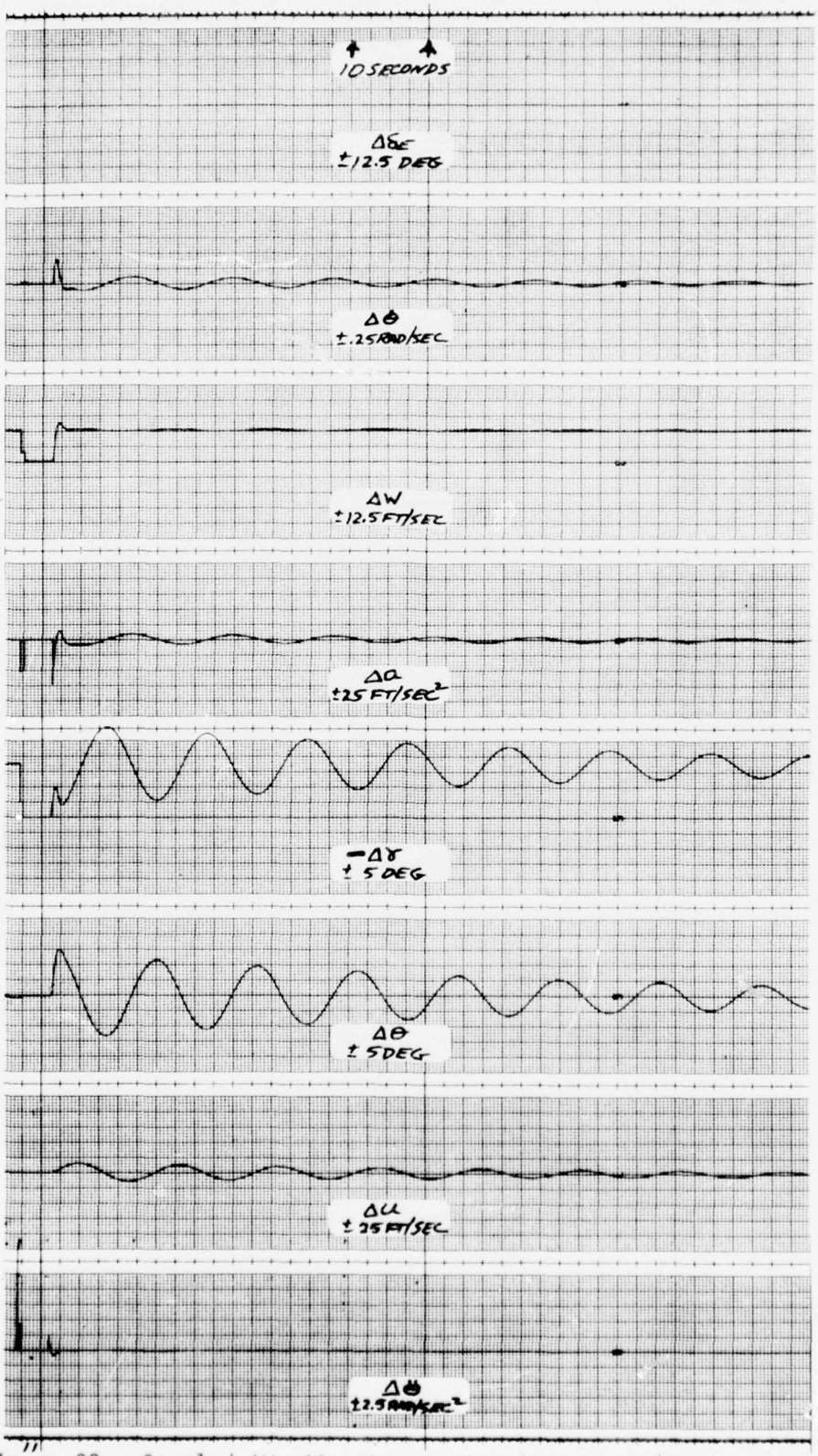

Figure 22. Coupled ΔW, $\Delta\theta$, ΔU response to a gust input (ΔW_G = -5 ft/sec)

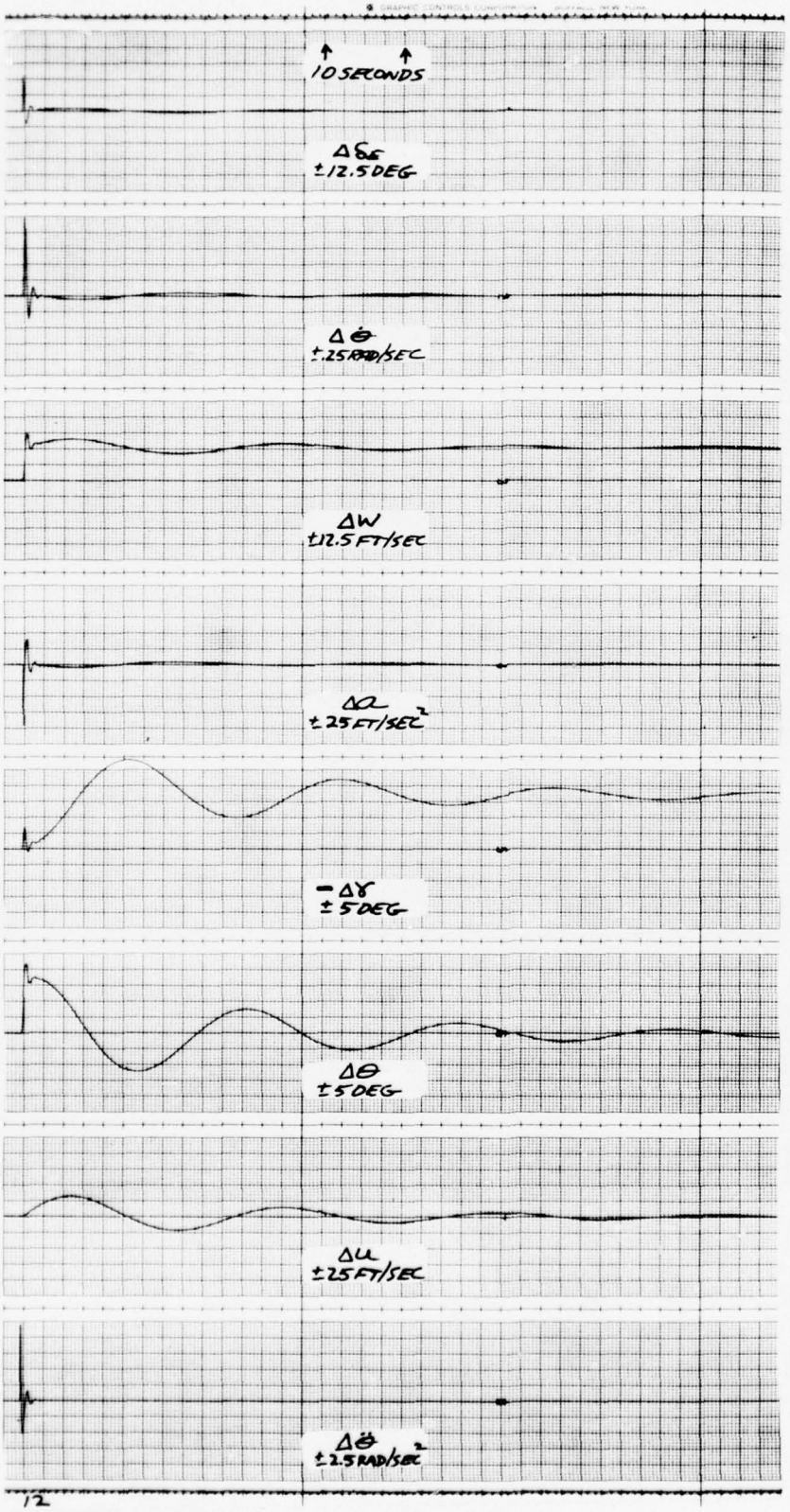

Figure 23. Augmented response (K_a = -0.007 to a gust input (ΔW_G = 5 ft/sec)

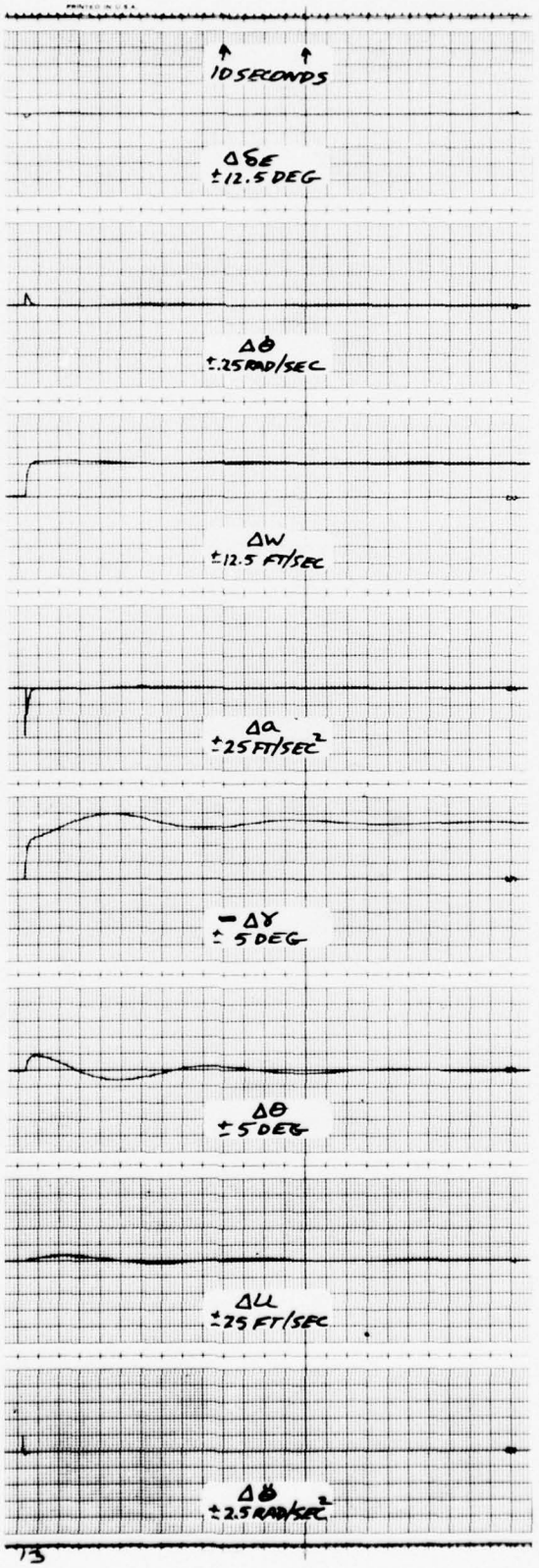

Figure 24. Augmented response (K_θ = -0.35) to a gust input

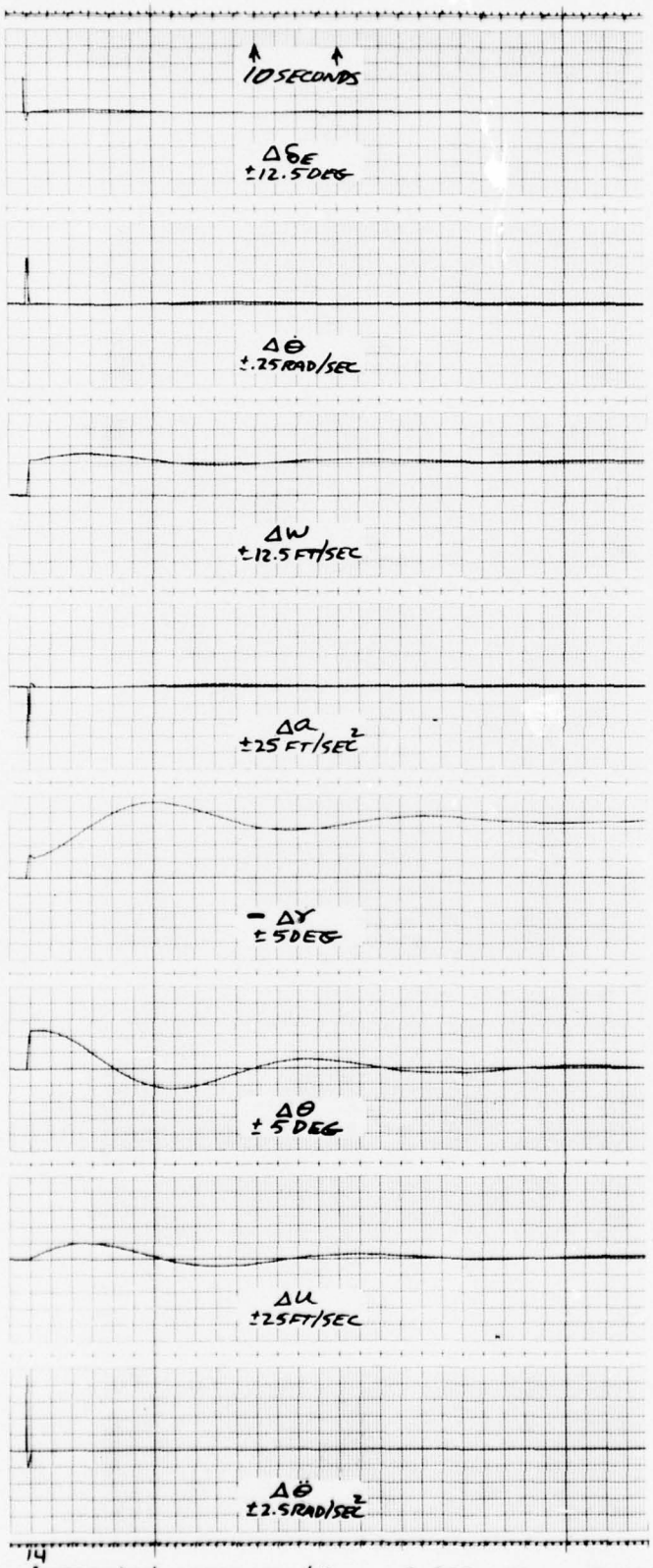

Figure 25. Augmented response (K_a = -0.007, $K_{\dot{\theta}}$ = -0.35) to a gust input

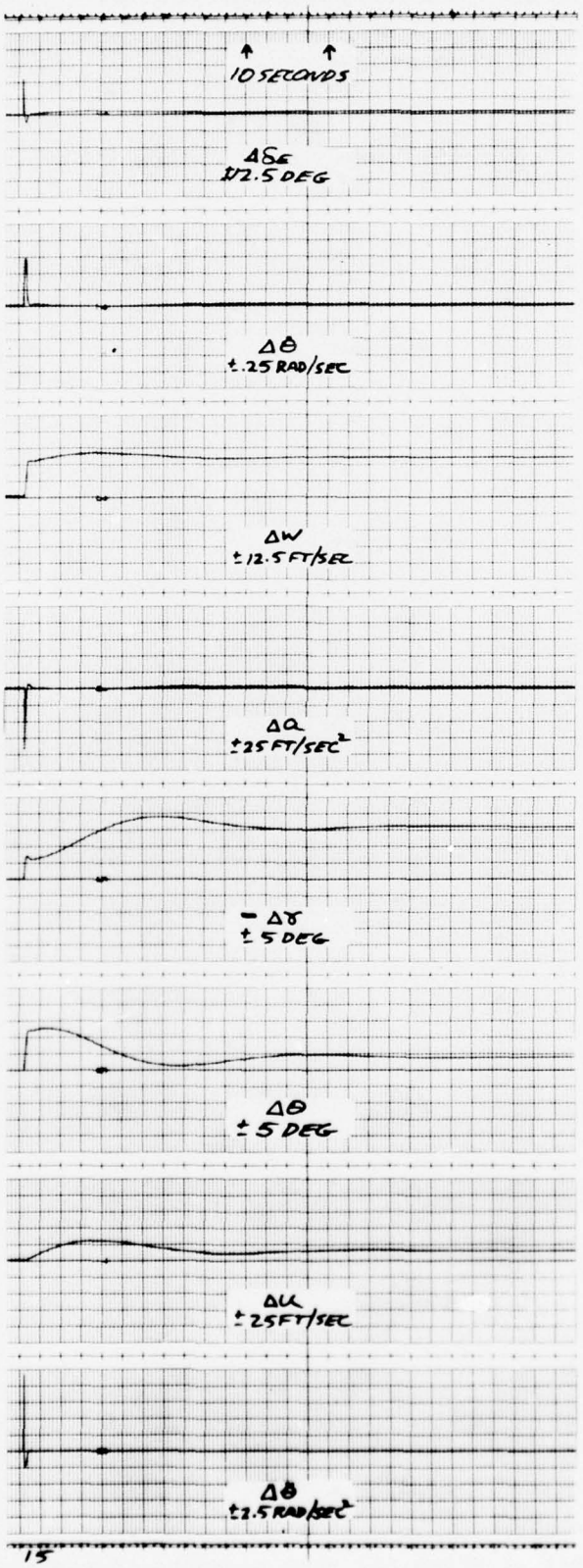

Figure 26. ΔW_G gust response (K_a = -0.007, $K_{\dot{\theta}}$ = -0.35, K_I = -0.0007)

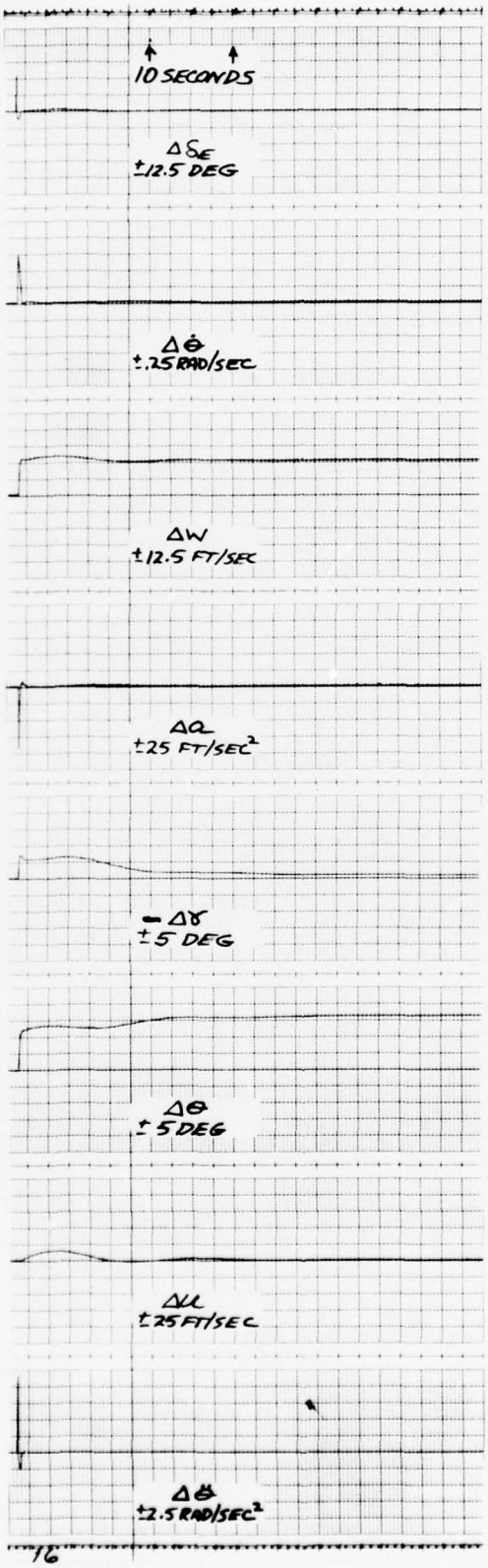

Figure 27. Autopilot/airframe ΔW_G gust response (Appendix A, Figure A-4)

($\Delta W = \Delta W_A = \Delta\theta = 0$). This behavior is clearly shown in Figure 22 where one should recall that $\Delta W_A = \Delta W + \Delta W_G$ and that $\Delta\gamma$ being nonzero is consistent with the stated aerodynamic trim of the aircraft. The incorporation of an autopilot may or may not modify the behavior described above. The autopilot feedback (5.23) is transient in nature so that the stabilized airframe (Figure 25) also returns to the original aerodynamic trim. If the autopilot incorporates a pitch trim integrator such as,

$$\Delta\delta_E = K_a\,(\Delta a_C - \Delta a) - K_{\dot\theta}\,\Delta\dot\theta + K_I \int_0^t (\Delta a_C - \Delta a)\,dt \qquad (5.38)$$

then the long term behavior of the aircraft is modified as $\Delta\delta_E$ is nonzero in the steady state (Figure 26). It is the opinion of this author that caution be exercised in the use of low frequency feedbacks in a necessarily responsive autopilot channel. Error or trim integrators such as 5.38 are the least offensive form of these type feedbacks but the general feeling still applies. The feedbacks can have a beneficial effect on the long term stability of the airframe (e.g., note the increased phugoid damping of Figure 26 compared with Figure 25), but such effects can also be obtained by guidance phenomena (λ, $\dot\lambda$, etc.). To retain the conservative framework, expression 5.38 is used as the acceleration autopilot feedback for the remainder of the simulation traces (see Appendix A for the complete autopilot representation). Figure 27 depicts the gust response of the complete autopilot/airframe system.

6. COUPLED GUIDANCE AND CONTROL FUNCTIONS

The approach taken thus far has been to treat the guidance function and the control function in an independent fashion. This does not imply that the potential of coupling between the guidance dynamics and the control dynamics has been ignored. The near-field gain limiting was incorporated into the guidance law to achieve compatibility between the guidance dynamics and the autopilot/airframe dynamics. The simulation effort will be completed by the merging of these two functions.

Figure 28 is similar to Figure 13 with the exception that the commanded normal acceleration (Δa_C) and the commanded airspeed (ΔU_C) are filtered by the airframe/autopilot dynamics before computation of the guidance kinematics (λ, $\dot\lambda$). Since the guidance gain is not limited ($R_m = 0$), the expected near-field flight path instability is produced. For the autopilot implementation of Figure A-4, the range at which the instability occurs is on the order of 300 feet for the chosen n = 15. One might now expect to see a stability analysis of the guidance law (4.4) and the $\Delta U = 0$ approximation to the stabilized airframe (5.19). Unfortunately, this stability analysis is not so easy. The system of equations depicted by Figure 28 is linear , but due to the time-varying coefficients produced by the constantly decreasing range, an analytical treatment is really quite difficult and fortunately unnecessary. The near-field gain control eliminates the analytic difficulties by conversion of the measured angular information (λ, $\dot\lambda$) to its equivalent (h_E, $\dot h_E$) and stabilization of the system gain at the R_M value. More importantly, proper adjustment of the gain control will be seen to eliminate the instability along with the associated analytic difficulties.

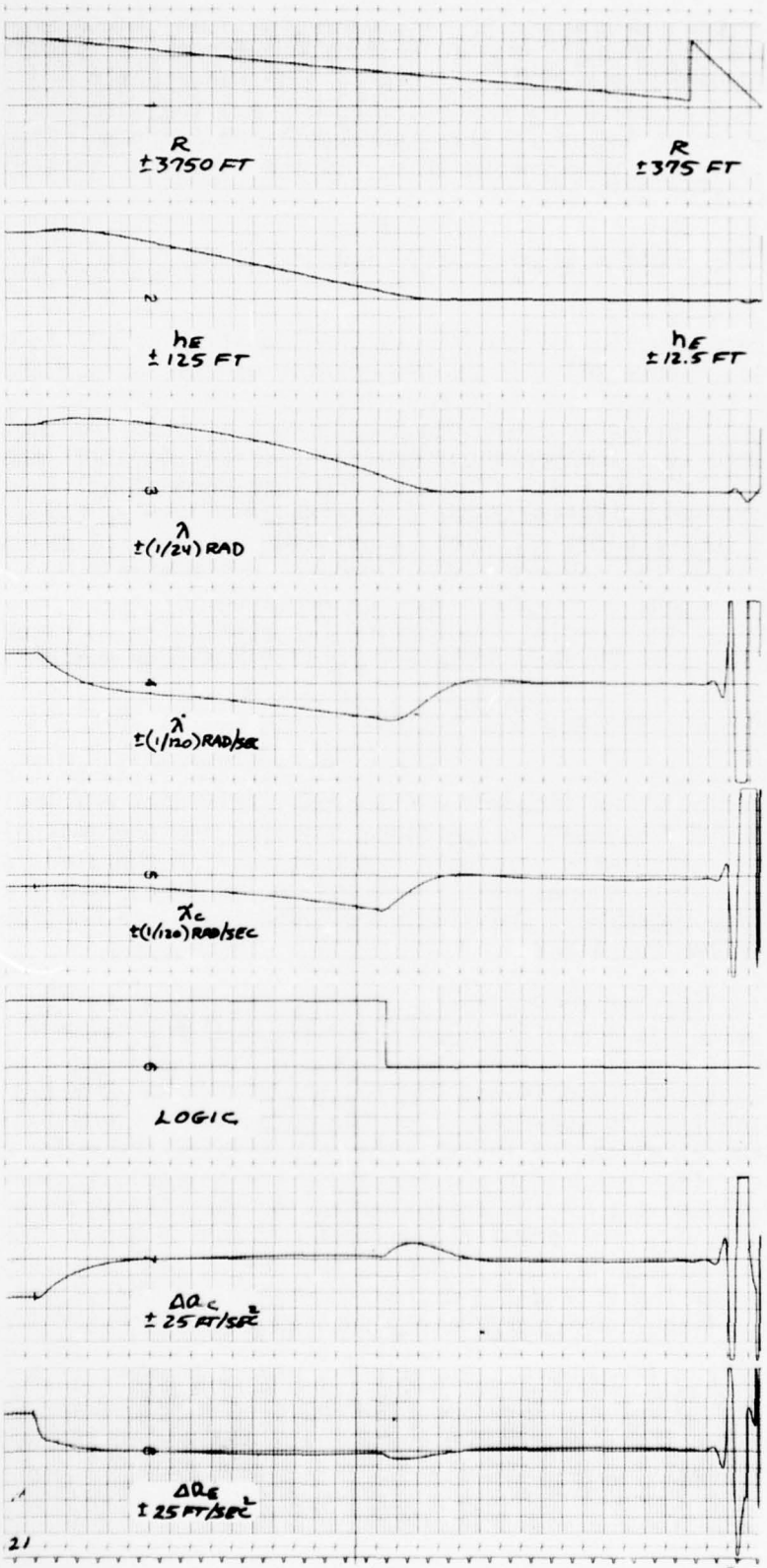

Figure 28. Coupled guidance response (n = 15, R_m = 0, $\gamma_L = 8^o$, $\gamma_F = 4^o$)

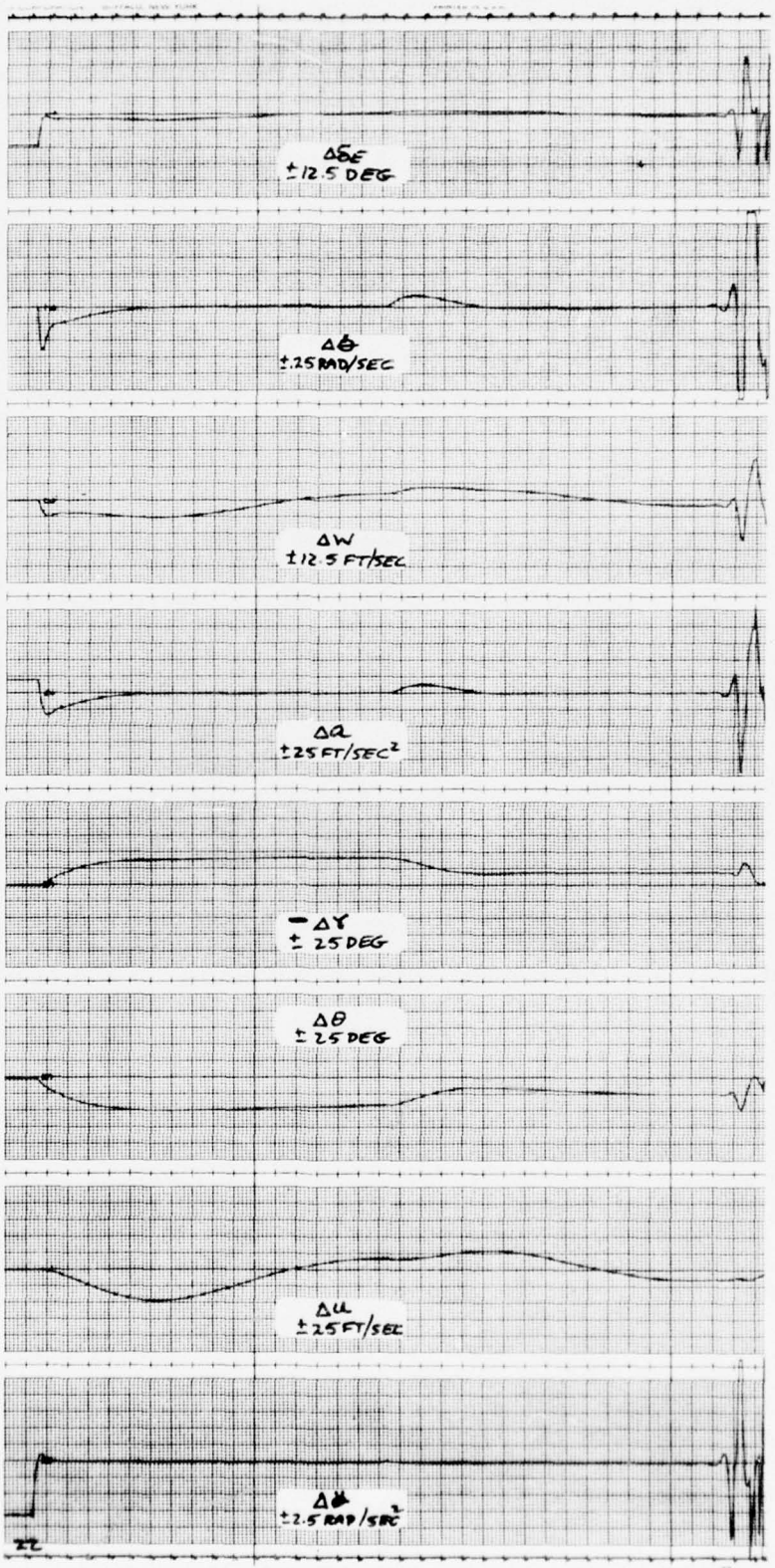

Figure 29. Coupled control response ($n = 15$, $R_m = 0$, $\gamma_L = 8^o$, $\gamma_F = 4^o$)

Figures 30 and 31 depict the gust response of the coupled system with gain limiting (R_m = 300 ft). As in Section 3, the system is perturbed (R_D = 600 ft) from its initial trim on the glide slope. The instability is still in evidence though its severity is bounded by the gain limiting (R_m = 300 feet to touchdown. To provide some gain margin for the autopilot configuration of Figure A-4, the design value for the gain parameter (R_m) was chosen to be 1,000 feet.

The coupled response of the design configuration (n = 15, R_m = 1,000 ft) is given in Figures 32 and 33. The idealized guidance response ($\Delta a = \Delta a_c$) was previously given in Figure 13. The most apparent difference between the two figures is the low frequency drift (Δa_c, Δa_e) of Figure 32. This phenomenon is the result of the trim integrators previously mentioned and more quantitatively depicted in the $\Delta\delta_E$ trace of Figure 33. Comparison of the Δa and Δa_c traces demonstrate that a successful approach is not dependent upon holding Δa_e near zero. As a matter of interest, the reader should also note the effective control of descending flight path angle ($|\gamma| \leq 8^o$) by command limiting of $\dot{\lambda}$.

Figures 34 through 37 depict the coupled guidance and control responses of the design configuration to a ΔW_G gust input (R_D = 600 and 300 feet, respectively. In both cases, the peak Δh_E was one (1) foot. The invarient Δh_E perturbation is consistent with the concept of a constant gain system for all ranges less than R_m = 1,000 feet. The worst case computations of Section 3 ($\Delta\theta$ = 0) indicated a peak Δh_E of 1.5 feet (e.g., See Figures 11 and 12). The difference is due to the gust alleviation properties of the stabilized airframe.

7. SUMMARY OF CONCLUSIONS

The efforts of the preceding six sections have tried to indicate a suggested direction for the design of an RPV approach guidance and control system. Every effort was made to maintain a conservative framework for the nominal design configuration developed within those six sections. As a result, it is felt that the performance of the concept can be significantly improved by a detailed stability and control analysis, particularly in the near-field region with the intent of selecting optimum values for the parameters (R_m, n, K_a, $K\dot{\theta}$) for use with a specific RPV airframe/engine design. The more pertinent results of the effort of the first six sections follow.

a. An approach guidance law was developed which was felt to have application to the general problem of IFR landing of aircraft of any type. For continuous measurement of the angular deviation of the aircraft from the glide path (γ), its time rate of change ($\dot{\lambda}$) and the horizontal range (R) of the aircraft from the landing site, the guidance law was shown to have inherent stability even as the range approaches zero. To achieve this inherent stability, the bandwidth of the guidance law is required to vary as R^{-1}.

b. To compensate for the effects of lags in the response of the airframe to the guidance law demands, a near-field gain control was incorporated. This gain control was shown to limit the bandwidth of the guidance law for $R \leq R_m$ to a value compatible with the airframe's ability to respond. The guidance law bandwidth must also be compatible with the data rate and noise spectra associated with measurement of λ, $\dot{\lambda}$, and R. In many applications, a direct measurement

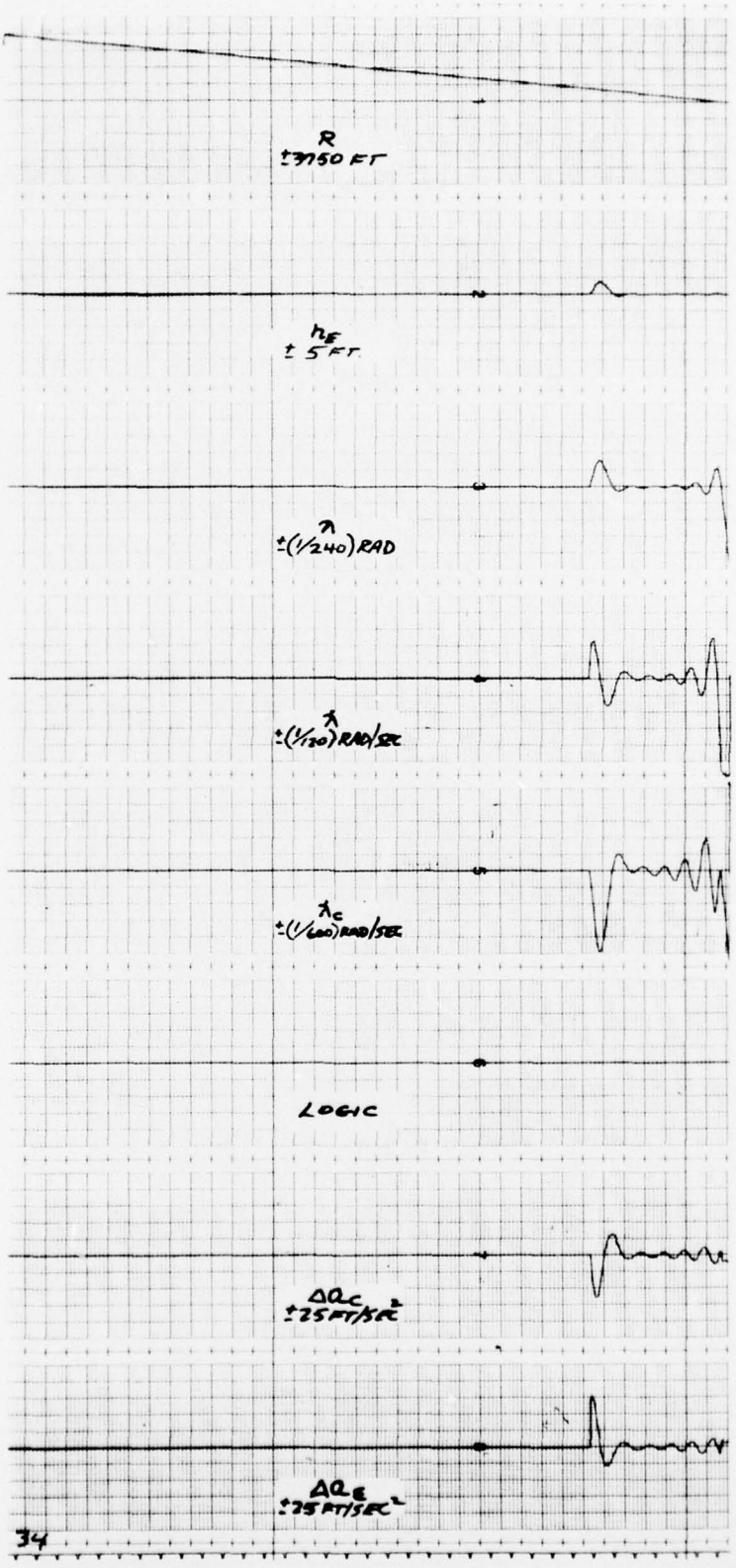

Figure 30. Coupled guidance response (n = 15, R_m = 300 ft, $\gamma_L = 8^o$, $\gamma_F = 4^o$, ΔW_G = 5 ft/sec, R_D = 600 ft)

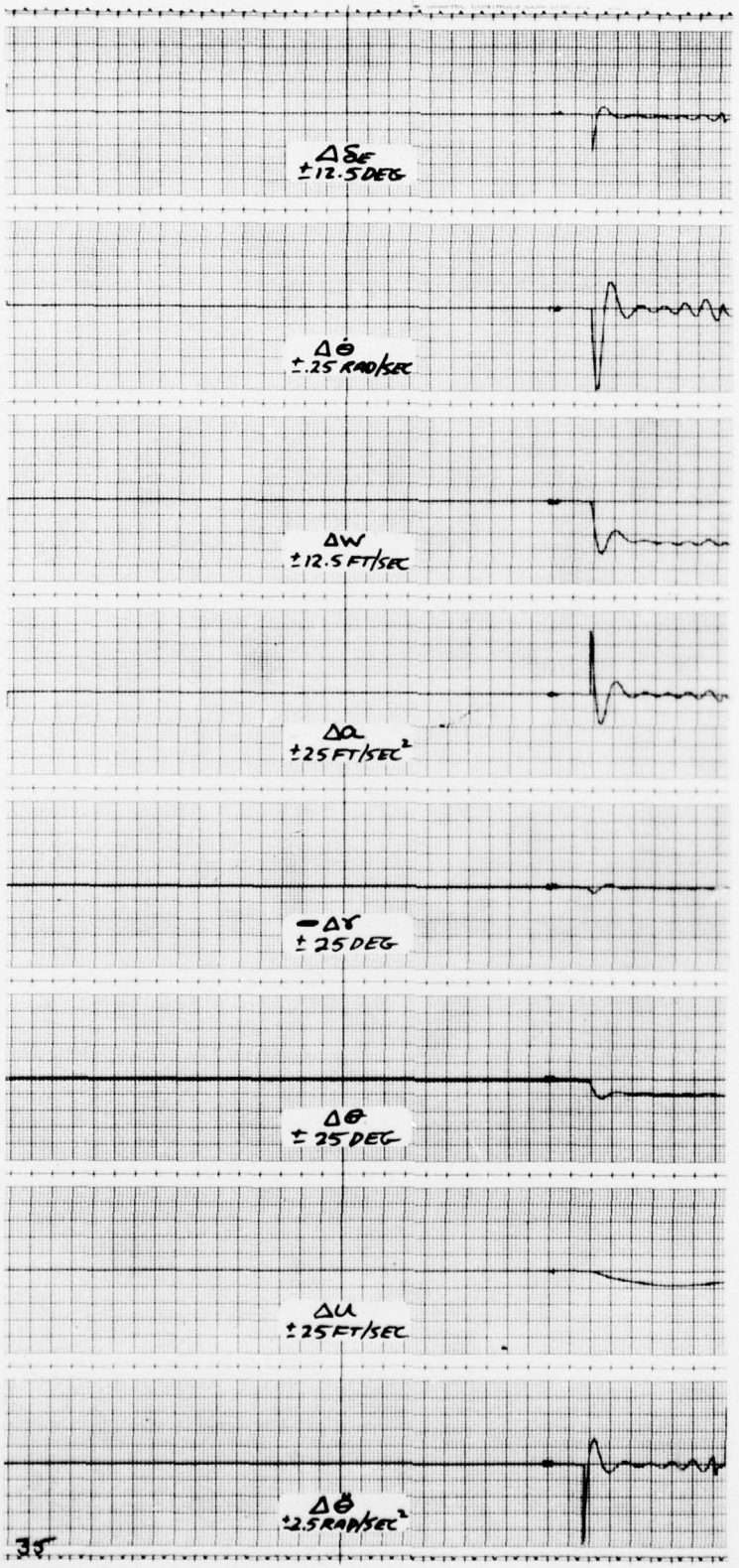

Figure 31. Coupled control response (n = 15, R_m = 300 ft, $\gamma_L = 8^o$, $\gamma_F = 4^o$, ΔW_G = 5 ft/sec, R_D = 600 ft)

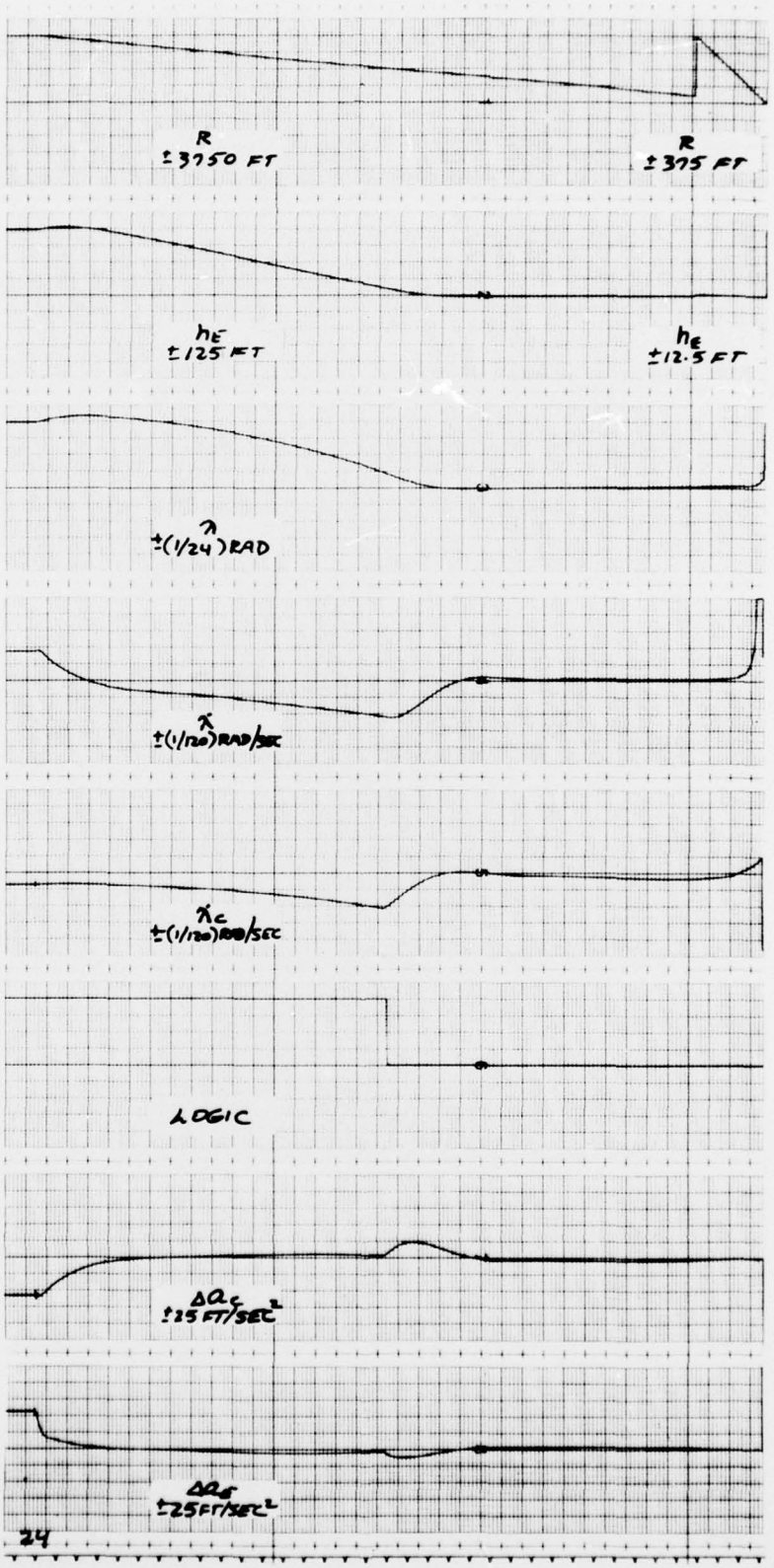

Figure 32. Coupled guidance response (n = 15, R_m = 1000 ft, $\gamma_L = 8^o$, $\gamma_F = 40$)

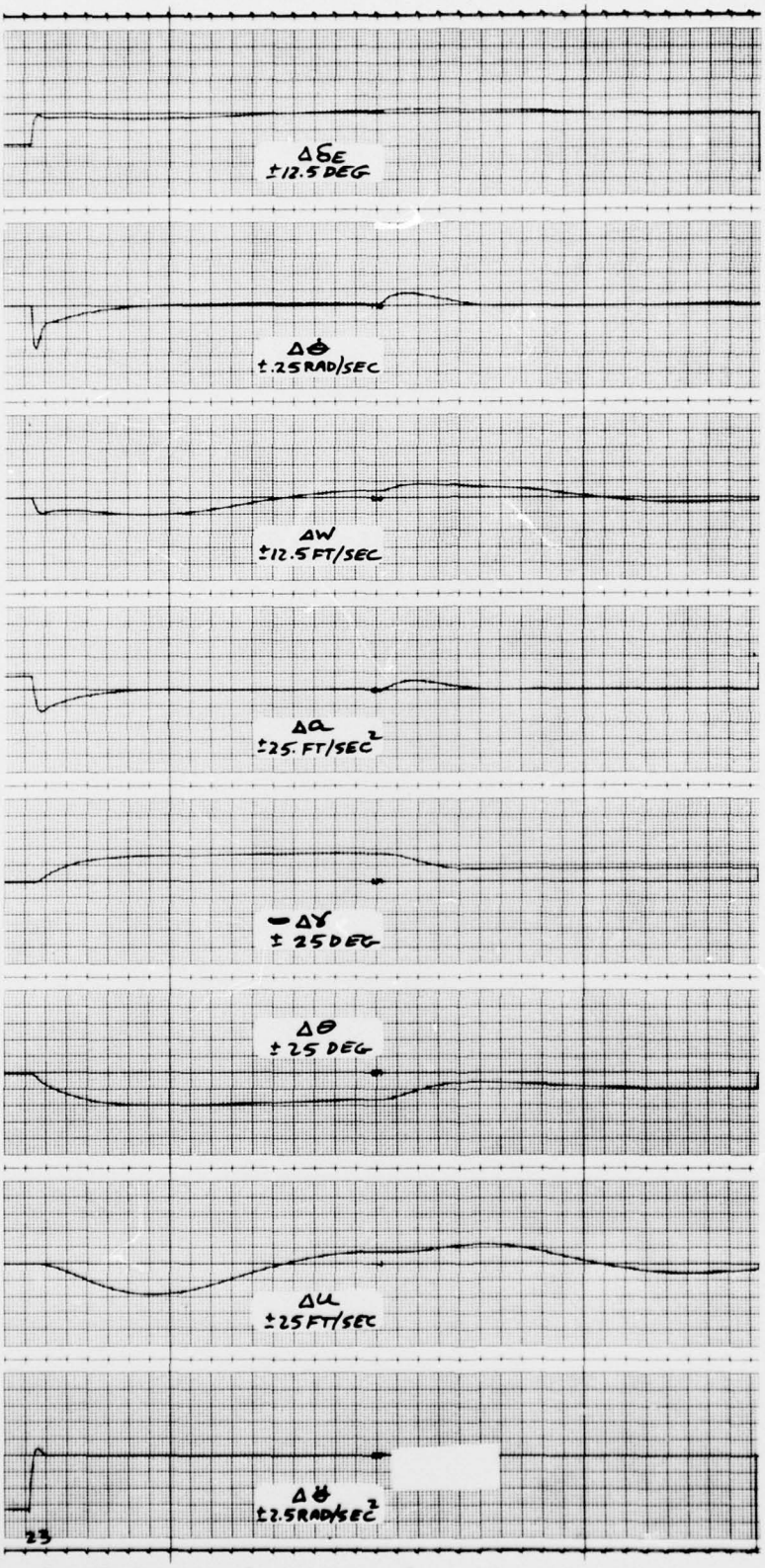

Figure 33. Coupled control response (n = 15, R_m = 1000 ft, $\gamma_L = 8^o$, $\gamma_F = 4^o$)

Figure 34. Coupled guidance response (n = 15, R_m = 1000, γ_L = 8°, γ_F = 4°, ΔW_G = 5 ft/sec, R_D = 600 ft)

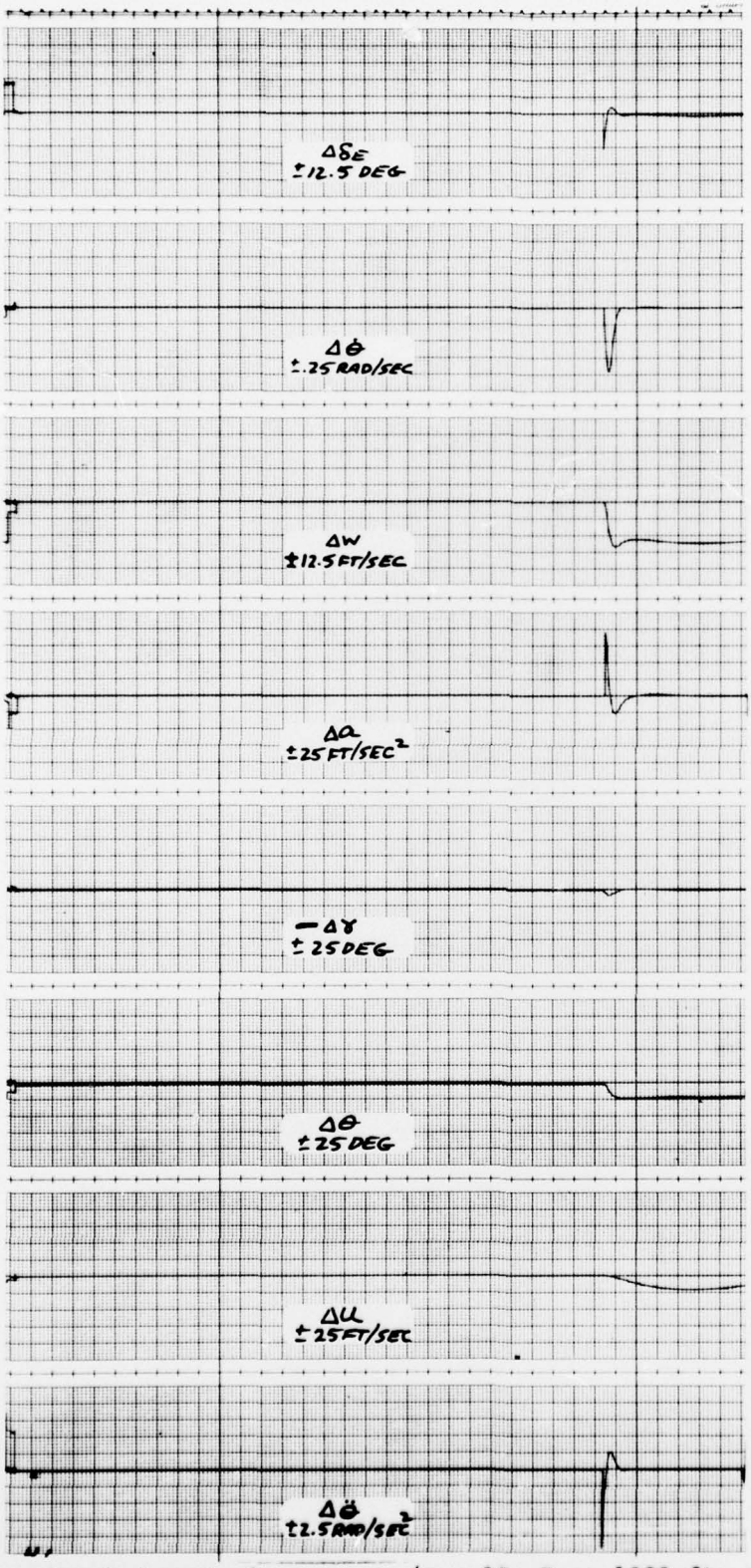

Figure 35. Coupled control response (n = 15, R_m = 1000 ft, $\gamma_L = 8^o$, $\gamma_F = 4^o$, ΔW_G = 5 ft/sec, R_D = 600 ft)

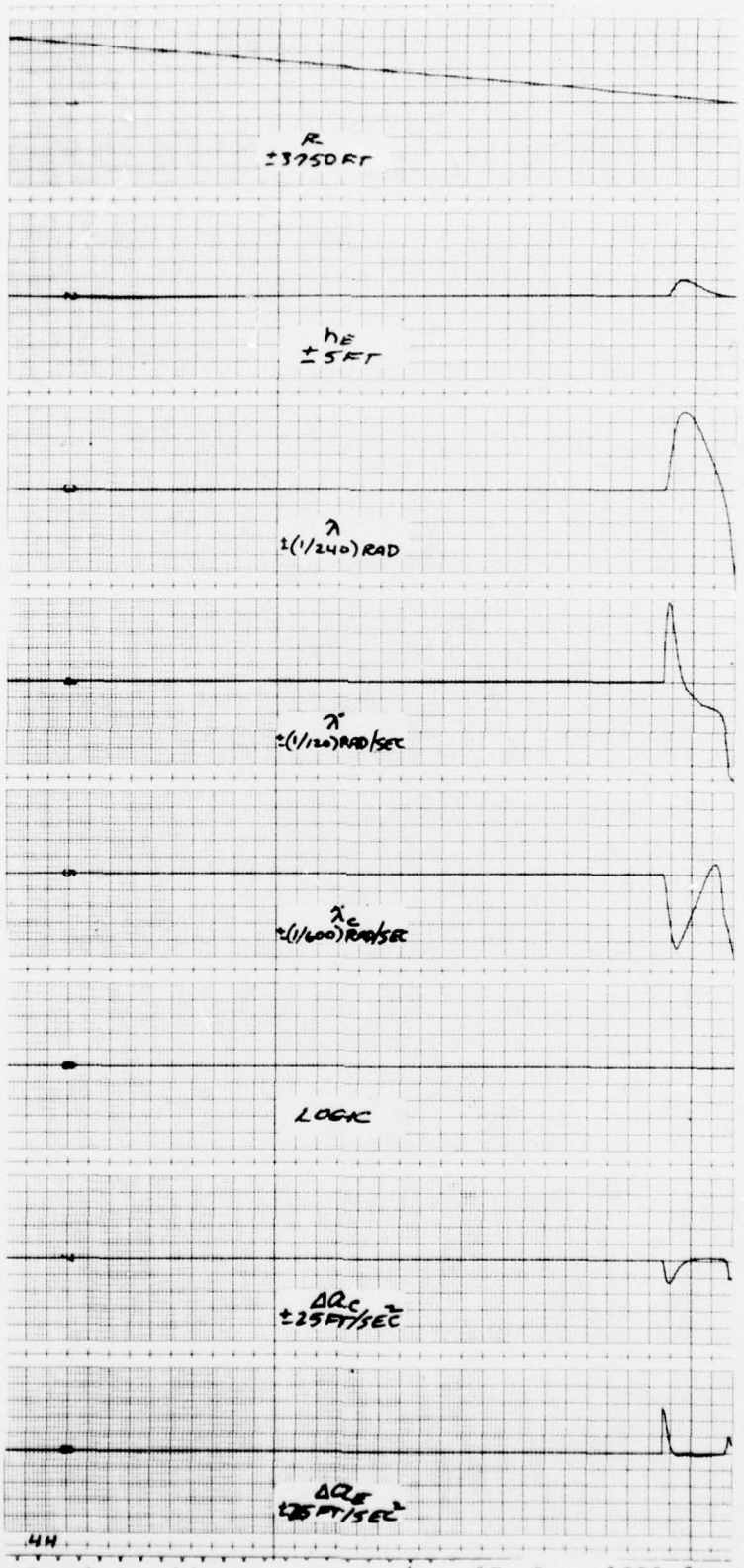

Figure 36. Coupled guidance response (n = 15, R_m = 1000 ft, $\gamma_L = 8^0$, $\gamma_F = 4^0$, ΔW_G = 5 ft/sec, R_D = 300 ft)

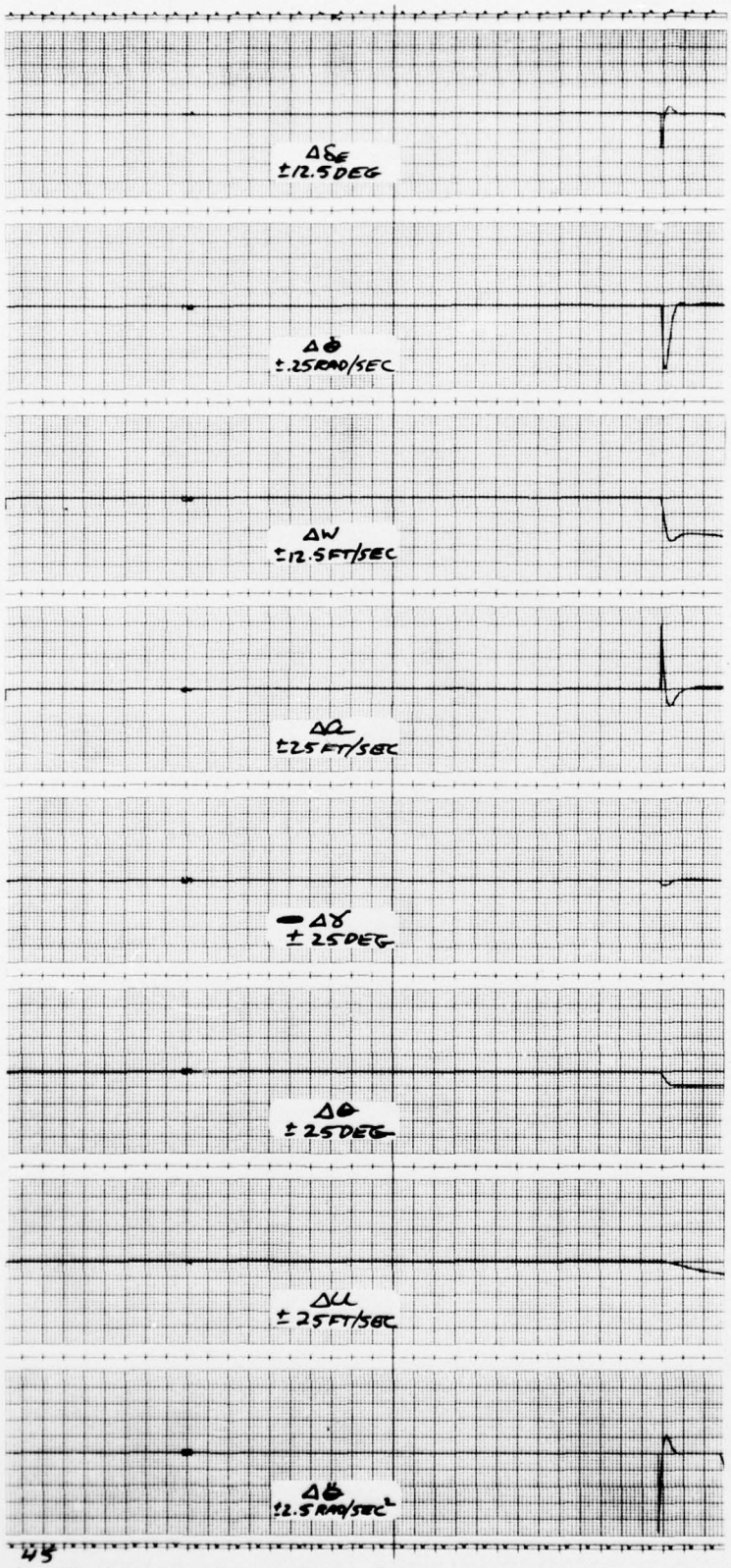

Figure 37. Coupled control response (n = 15, R_m = 1000 ft, γ_L = 8°, γ_F = 40, ΔW_G = 5 ft/sec, R_D = 300 ft)

of $\dot{\lambda}$ will not be available. System performance (i.e., guidance law bandwidth) will therefore be influenced by one's ability to approximate $\dot{\lambda}$ within the desired frequency region by operating upon the measured value of λ.

c. The near-field ($R < R_m$) gust response characteristics of the guidance law were quantitatively related to the guidance parameters R_m and n, and equivalently, to the bandwidth of the guidance law. This analytic treatment, which neglected airframe dynamics, was shown to represent a worst case situation due to the gust alleviation properties of the stabilized airframe.

d. Command limiting ($\dot{\lambda}_c$) within the guidance law was shown to provide an effective control over the maximum angle of descent when a measurement of flight path angle (γ) is not available. The command limiting is necessary to avoid a build-up of airspeed under flight-idle engine conditions. The technique may also be applied to climbing flight to avoid conditions of insufficient power available, but this application was not considered in this simulation effort.

e. A very simple "approach autopilot" concept was suggested for the mini-RPV landing function. The autopilot relies on normal acceleration and pitching rate feedbacks to control and stabilize the short period and phugoid modes of airframe motion.

An attempt has been made within this document to carefully distinguish between the guidance function and the control function. The intent was to clearly discriminate the design objectives of each. When one considers the physical mechanization of the two functions, however, there is no associated implication that the two be clearly discernable (e.g., guidance calculations in a ground-based computer, control calculations within the air vehicle). Most certainly, the minimum required airborne computation is that associated with the control function. With the advent of microprocessor technology, however, one is inexorably drawn toward centralization of the guidance and control calculations in what should be referred to as an "Approach Guidance and Control Computer." The inputs to the computer would be communicated λ and R from the ground based radar or optical tracker, and the airframe normal acceleration and pitching rate from the airborne sensors. The outputs of the computer would be electrical signals to drive the control surface sensors (i.e., a "digital autopilot") for an RPV application, or to drive a flight director for the IFR, piloted application.

APPENDIX

This appendix contains the scaled analog simulation diagrams for the airframe, auto-pilot, and associated kinematic relationships.

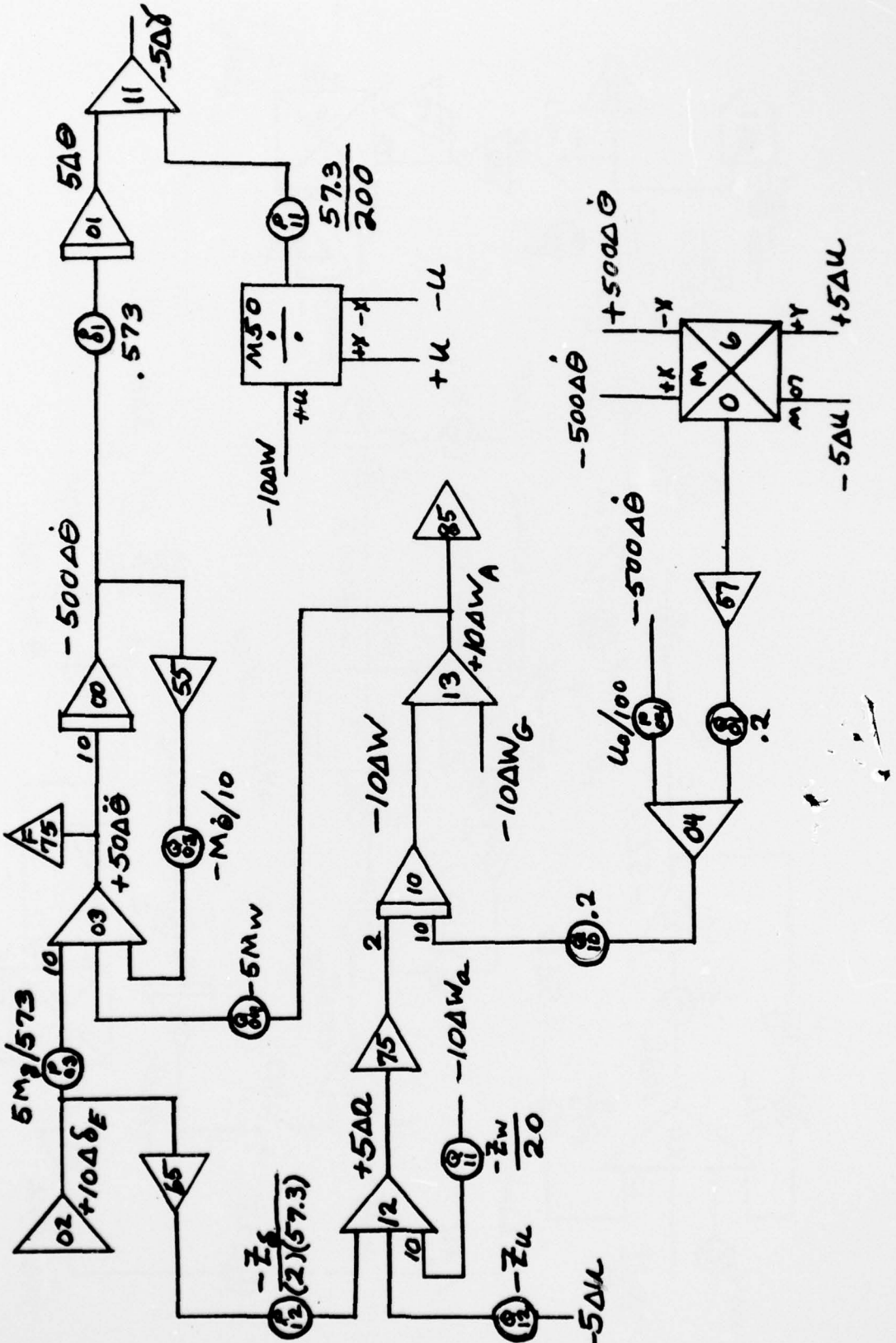

Figure A-1. Short period airframe dynamics

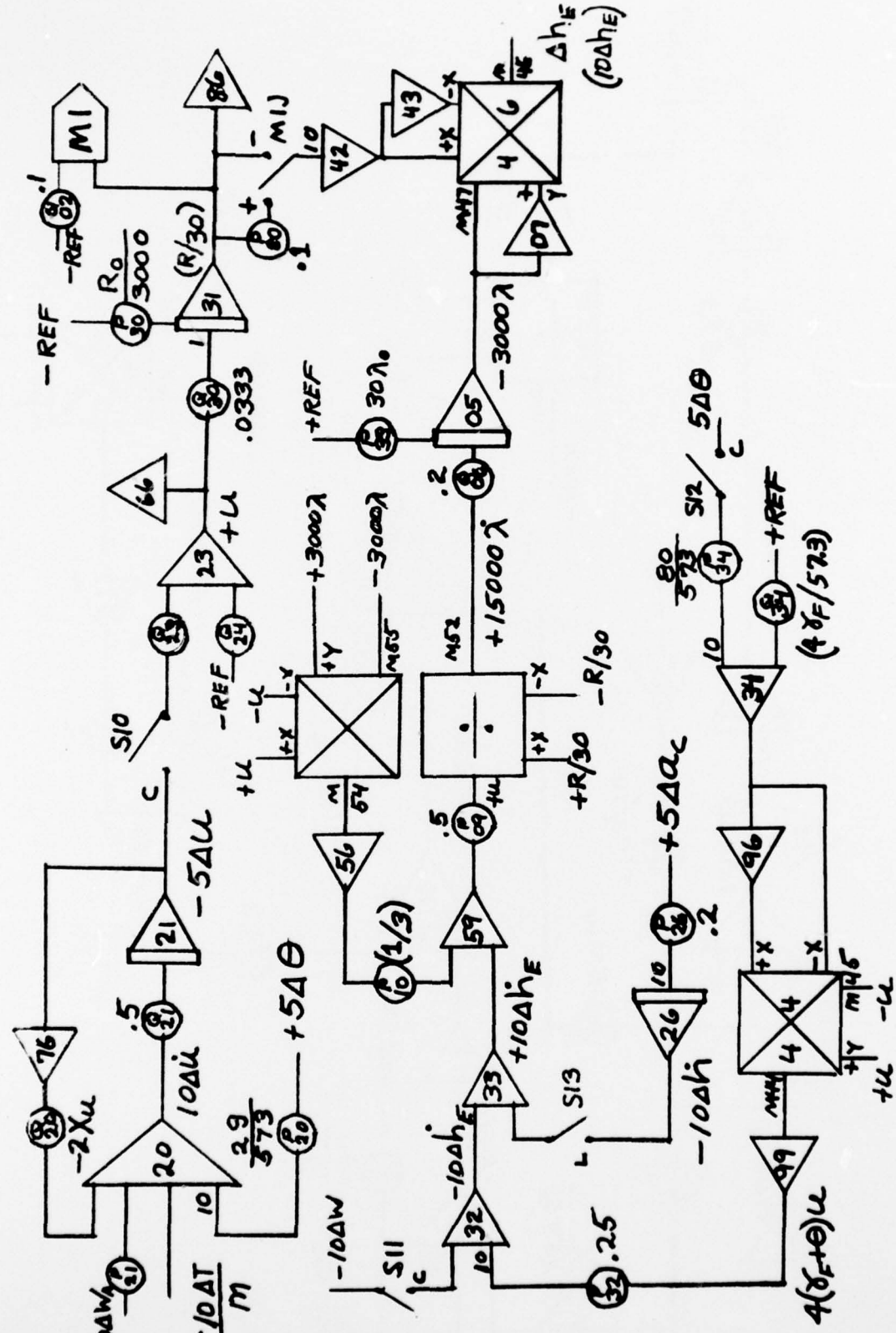

Figure A-2. Phugoid airframe dynamics and kinematics

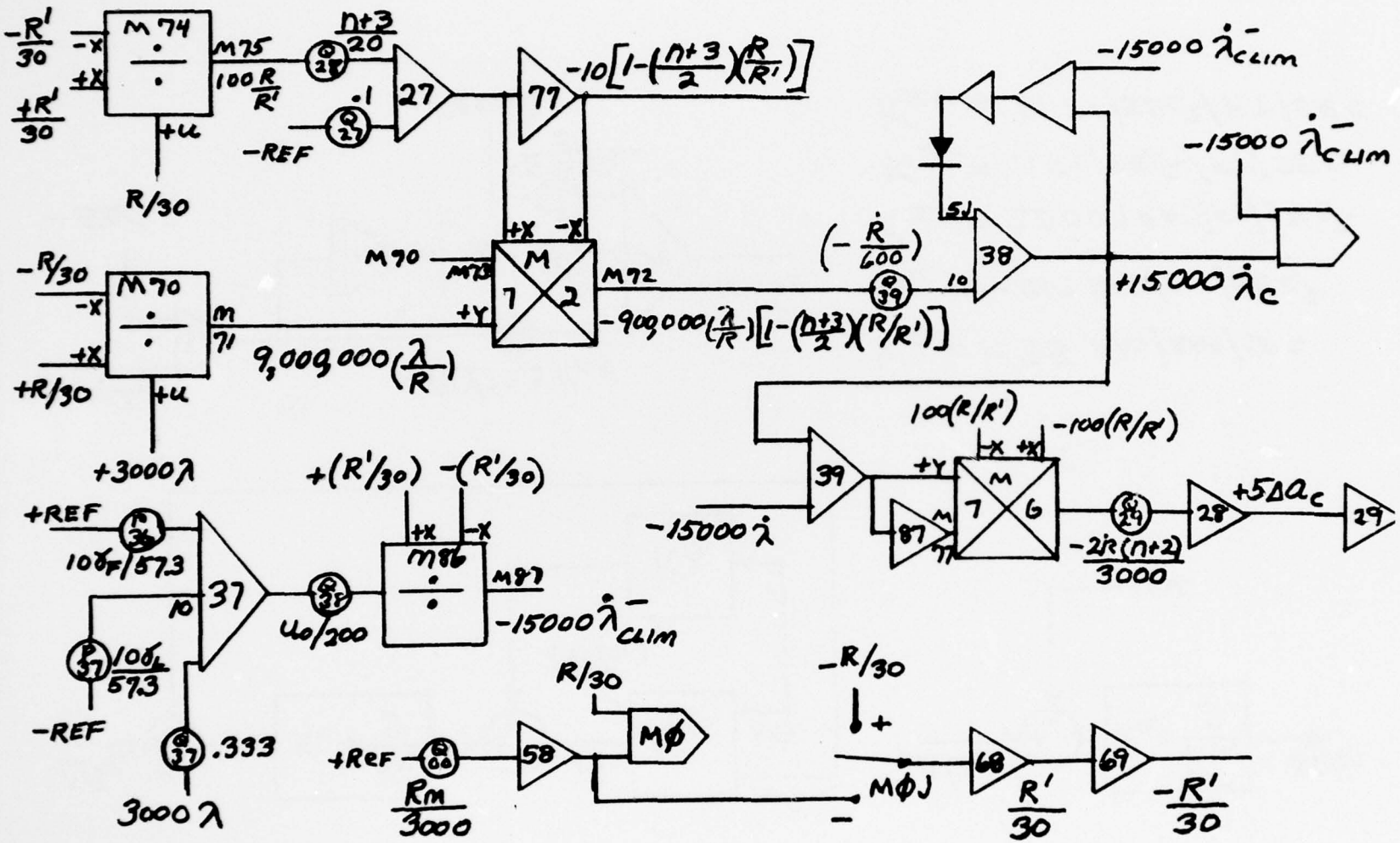

Figure A-3. Guidance formulation including gain and path angle limiting

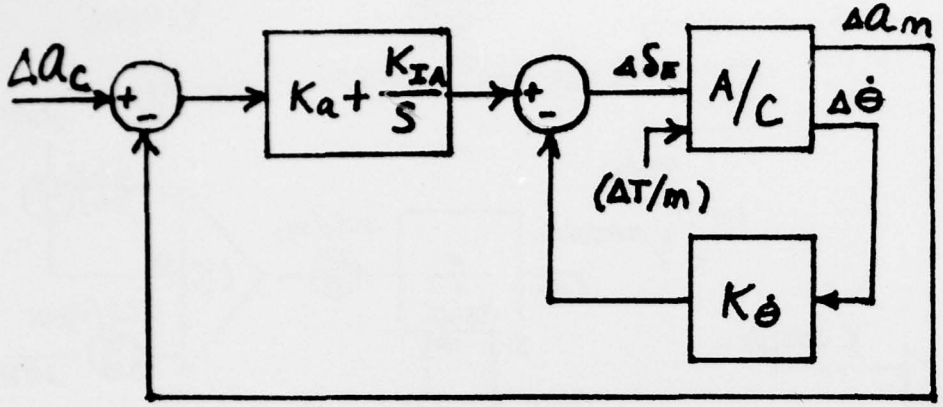

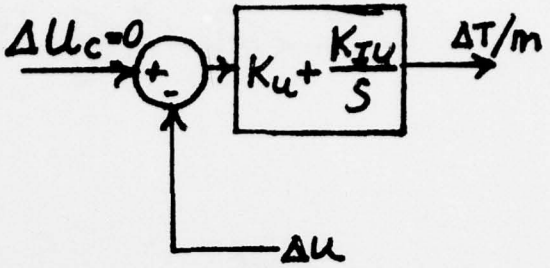

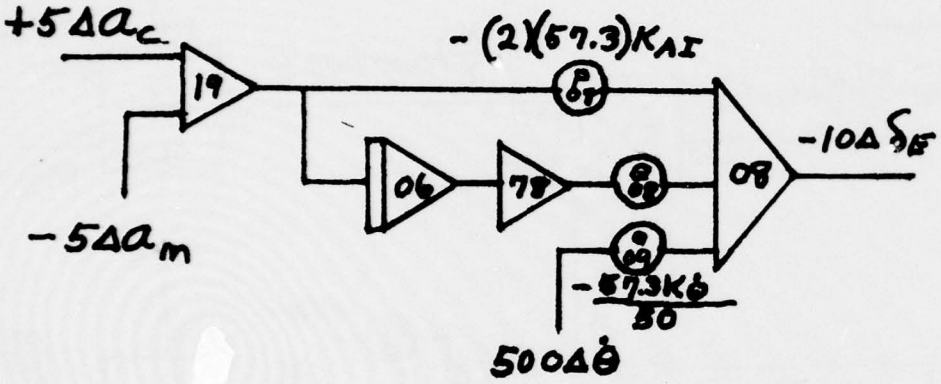

$K_{\dot{\theta}} = -.35$ RAD/RAD/SEC

$K_a = -.007$ RAD/FT/SEC^2

$K_{IA} = -.0007$ RAD/FT/SEC^2

$K_u = .1$ FT/SEC^2/FT/SEC

$K_{IU} = .01$ FT/SEC^2/FT/SEC

Figure A-4. Autopilot representation